Bulletin of the Seismological Society of America, Vol. 102, No. 3, pp. 1059–1078, June 2012, doi: 10.1785/0120110103

Paleoseismicity of the Southern End of the Cascadia Subduction Zone, Northwestern California

by David W. Valentine, Edward A. Keller, Gary Carver, Wen-Hao Li, Christine Manhart, and Alexander R. Simms

Abstract The southern end of the Cascadia subduction zone (CSZ) in northwestern California poses a high seismic hazard. This study uses the Quaternary stratigraphy of the bays and estuaries to reconstruct coseismic subsidence caused by strong to great earthquakes. We used lithology, macrofossils, and microfossils to estimate the amount of relative sea-level change at contacts caused by coseismic subsidence. Our paleoseismic record contains evidence of four to six earthquakes over the past 2000 years. Using the pattern and magnitude of submergence and other paleoseismic information (trenches and other sites), we determine whether the earthquakes were local or regional. We found that the record contained evidence for both smaller strong to major earthquakes on local structures (M_w 6.5–7.2) and larger regional subduction-zone-related great earthquakes ($M_w > 8.2$). We compared our record to other records from Oregon and Washington and found three earthquakes likely caused by the rupture of the entire CSZ around approximately 230–270 (the A.D. 1700 event), 1150–1400, and 1750–1900 cal B.P. In addition, two other local earthquakes likely occurred around 500–600, 1000–1250, and possibly 1500–1650 cal B.P.

Online Material: Table of radiocarbon ages obtained in the study.

Introduction

Prior to the works of Heaton and Kanamori (1984) and Atwater (1987), the earthquake and tsunami threat along the Cascadia subduction zone (CSZ) was classified as minimal (see Clague, Atwater, *et al.*, 2000; Fig. 1). However, recent work continues to confirm the occurrence of large earthquakes and associated tsunamis and turbidites along the entire length of the CSZ from southern British Columbia (Clague, Bobrowsky, and Hutchison, 2000; Goldfinger *et al.*, 2003) through Washington (Atwater, 1987, 1992; Atwater *et al.*, 2004; Shennan *et al.*, 1996), Oregon (Nelson *et al.*, 1996, 2006, 2008; Shennan *et al.*, 1998; Kelsey *et al.*, 2002, 2005; Witter *et al.*, 2003), and parts of northern California (Clarke and Carver, 1992; Jacoby *et al.*, 1995; Abramson, 1998). Despite this work, ambiguity remains concerning the nature of the earthquakes recorded within the many different archives of paleoseismicity from the region. In particular, better records of paleoseismicity along key portions of the subduction zone are needed. The northern California section of the CSZ has not been as well studied as the CSZ further to the north in Oregon and Washington. The purpose of this paper is to compile various datasets collected over nearly three decades, in particular the stratigraphy of Humboldt Bay and the Eel River delta, California, to reconstruct the earthquake history of the past 2000 years for the southern end of the CSZ. Our new record of earthquakes is compared to other paleoseismic studies further to the north to provide a better understanding of the length of rupture along the CSZ.

Setting and Approach

Study Area

Our study area is located along the northern California coast near the towns of Eureka and Arcata (Figs. 1 and 2). Northwestern California is one of the most seismically active regions of the United States (Dengler *et al.*, 1991). Most of the seismicity occurs on the Mendocino transform fault and faults within the deforming Juan de Fuca plate along the CSZ (Fig. 1). In addition, several faults and/or fault zones including the Little Salmon fault and Mad River fault zone on the western edge of the North American plate show evidence of Quaternary activity (Clarke, 1992; Fig. 2). However, whether movement on these faults is independent of, or associated with, movement on the CSZ megathrust is largely unknown. The only historic earthquake associated with the CSZ is the 1992 Cape Mendocino earthquake (M_w 7.1), which ruptured a small portion of the CSZ (Oppenheimer *et al.*, 1993).

The coastal tidal marshes, floodplains, and estuaries of Humboldt Bay and the Eel River floodplain and delta are

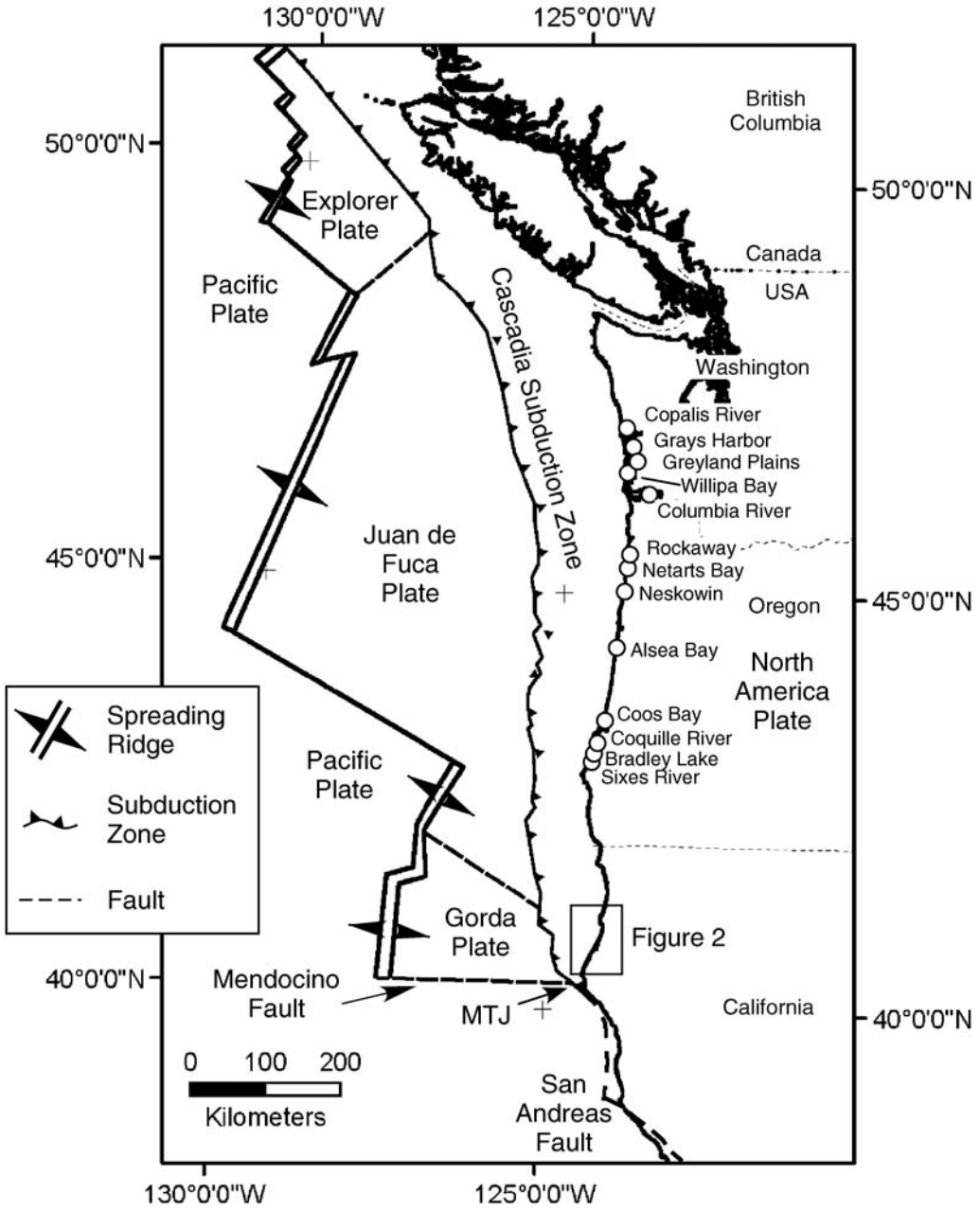

Figure 1. Map of the CSZ (modified from Nelson *et al.*, 2008; after Atwater and Hemphill-Haley, 1997). The sites shown in Figure 2 and other locations and large-scale geologic features are discussed in the text.

found within actively forming synclines at the southern end of the CSZ where it merges with the northern reach of the San Andreas fault zone to form the Mendocino triple junction (MTJ; Fig. 1). The current geologic structures associated with the MTJ began forming about 700 ka–1 Ma (Carver, 1992; Burger *et al.*, 2002). Most regional structures trend northwest; however, near the study area, some of the structures trend east–west (Fig. 2). Faults accommodate about 10 mm/yr of shortening (McCory, 1996), with about 70% of the Quaternary shortening occurring on the Mad River and Little Salmon fault zones. Clarke (1992) grouped the faults and folds of the offshore CSZ into four zones: a zone of north- to northwest-trending reverse and thrust faults, a zone of broad open folds, a zone of en echelon folds and thrust faults trending oblique to the overall structural grain, and slope-parallel folds and thrust faults. Our sample sites are located within the zone of en echelon folds and thrust faults and the zone of broad folding. These folds include the Freshwater, South Bay (informal) and Eel River synclines (Fig. 2).

Approach

Atwater (1987) first suggested conducting paleoseismic studies of the CSZ using the stratigraphy of tidal wetlands. In

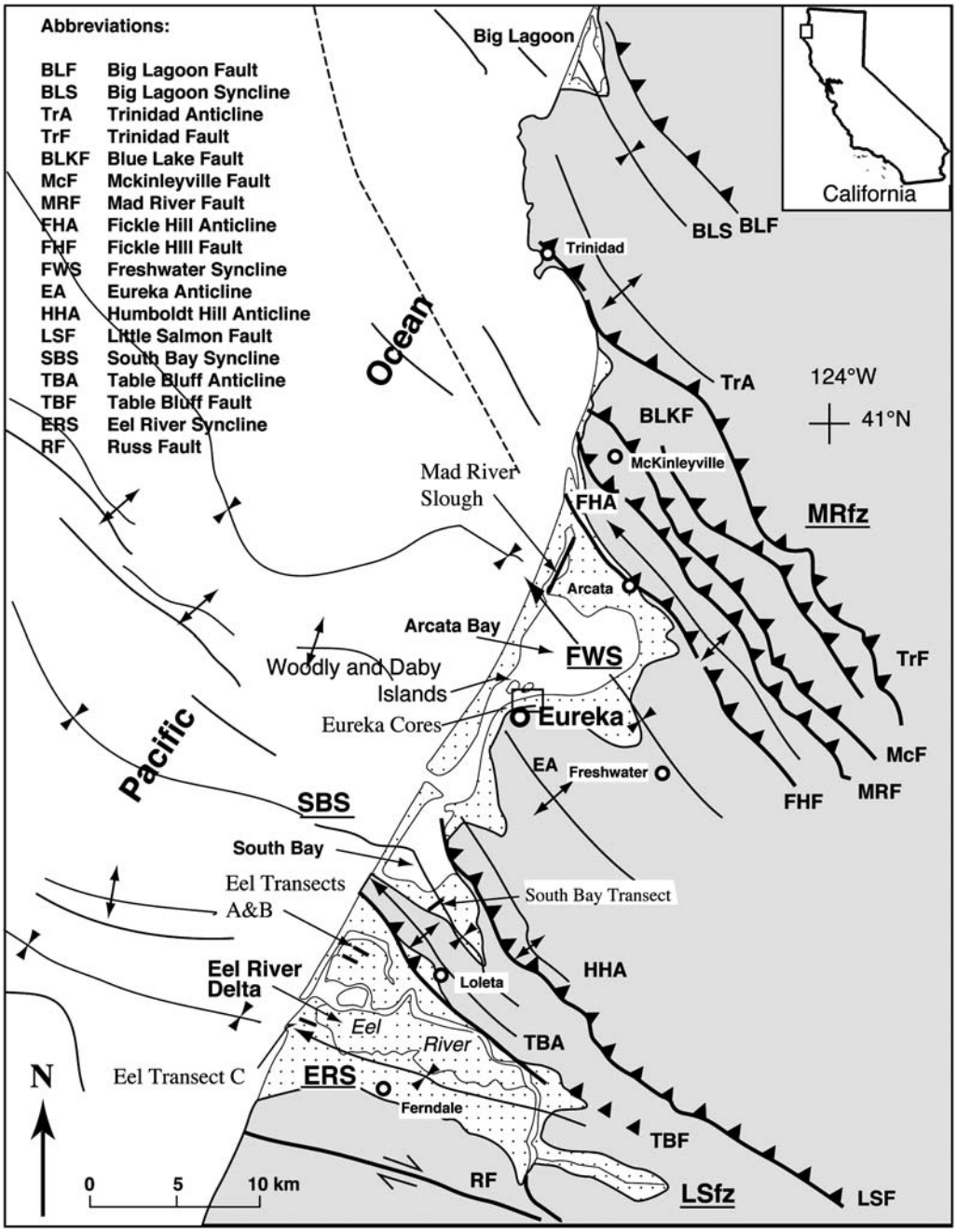

Figure 2. Map of the Eureka region showing the faults and folds located in the area and their proximity to our study sites. Map compiled from Clarke (1992), Clarke and Carver (1992), and references therein.

studies of Willipa Bay, Washington, sequences of tidal marsh and wetland soil beds buried by estuarine mud were interpreted as the result of coseismic subsidence (Atwater, 1987). Atwater's research suggested that during an earthquake, regional subsidence occurs, which submerges tidal-wetland surfaces. During the interseismic period, intertidal estuarine muds cover the surfaces, entomb plant fragments, and bury the marsh soil surface, creating peaty stratigraphic beds. Muddy sediment continues to accumulate until the surface attains an elevation at which marsh plants can colonize and begin the formation of tidal marsh surfaces and the associated peaty sediments. Since these first studies, work has continued to refine the criteria for identifying which peat burials were caused by coseismic subsidence versus other estuarine processes (e.g., eustatic and climatic water-level changes, and autocyclic changes such as tidal channel meander and local tidal changes caused by estuarine geometry changes; Atwater *et al.*, 1991, 2004; Nelson, 1992; Nelson *et al.*, 1996, 1998, 2006, 2008; Darienzo *et al.*, 1994; Shennan *et al.*, 1996, 1998; Kelsey *et al.*, 2002; Witter *et al.*, 2003; Hawkes *et al.*, 2010, 2011). At the southern end of the CSZ, within the present and former estuaries of Humboldt

Bay and the Eel River delta, the repeated tidal-wetland stratigraphy is probably formed by the same processes as the more well-studied peat stratigraphy further north, adjacent to the CSZ in Oregon and Washington (Li, 1992; Valentine, 1992; Vick, 1988).

For this study, the tidal marshes of Humboldt Bay were broken into three vertical zones, each representing about a 75 cm vertical elevation range, based on plant assemblages. These zones were largely defined by work conducted along the Mad River slough and include a low marsh, a transitional marsh, and a high marsh (Fig. 3; Eicher, 1987; Scott *et al.*, 1996). The modern marsh complex at Mad River slough is primarily dominated by three plant species: *Salicornia virginica*, *Spartina densiflora* (although not native but introduced in the late 1800s; Kittelson and Boyd, 1997), and *Distichlis spicata* (Eicher, 1987). The low marsh zone is defined as a *Salicornia* marsh and includes large dense mats of *Salicornia virginica* and individual clumps of *Spartina densiflora*. Occasionally, *Jaumea carnosa*, *Distichlis spicata*, and *Triglochin maritimum* are found in the low marsh zone. The transitional marsh zone is dominated by *Spartina densiflora* and contains a higher species diversity than the low marsh. The transitional marsh also contains *Salicornia virginica*, with fewer components of *Jaumea carnosa*, *Grindelia stricta*, and *Triglochin maritimum* (Eicher, 1987). The floral assemblage occupying the high marsh zone has the greatest diversity of any marsh zone. The dominant species are *Distichlis spicata* and *Salicornia virginica*. The high marsh consists of a meadow of grasses growing close to the ground with some higher plants. *Jaumea carnosa* was also found in small patches, as well as occasional clumps of *Spartina densiflora*.

In addition to these marsh species, the Humboldt Bay gum plant (*Grindelia stricta*) is an important relative sea-level (RSL) indicator. It is a rare plant with a highly dense woody root and has a vertical elevation range of about 0.2 m (Fig. 3; Eicher, 1987). Stratigraphic studies in Humboldt Bay (Vick, 1988; Valentine, 1992) use *Grindelia stricta* as a high marsh indicator fossil (Ia). *Grindelia stricta* is an extremely useful fossil because the root is easily preserved, and provides excellent material for carbon-14 (^{14}C) dating.

Foraminifer assemblage studies also aid in the assessment of RSL fluctuations. In order to determine the foraminifer assemblage composition of each of the modern marsh environments as defined by Eicher (1987) based on floral zones, we collected 15 samples from four transects of marshes around Humboldt Bay. Marsh floral assemblages and elevations were determined for each foraminifera sample location. Direct gradient, discriminant, and cluster analyses were applied to relate the foraminiferal assemblages to the floral assemblages. Then, using previously published elevations for "high," "transitional," and "low" marshes based on their flora (e.g., Eicher, 1987) as well as our measured elevations for each sample site, an elevation was applied to each foraminiferal assemblage. These foraminiferal assemblages were then used as analogs against which subsurface samples could be compared and the depositional environment

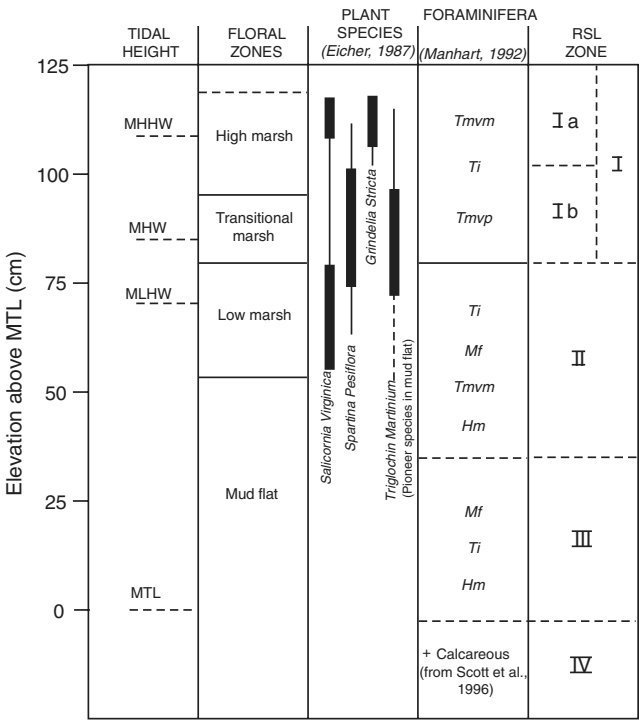

Figure 3. Vertical zonation of tidal marsh plants and foraminifera relative to mean sea level. These zones were used to establish the amount of RSL rise across each submergence event. The zones are delineated based on the presence or absence of the following species: Zone I: Foraminiferal assemblage zone dominated by *Trochammina macrescens* (Tmvm, macrescens var.; Tmvp, polystoma var.) and *Trochammina inflata* (Ti). When enough data are available, zone I may be split into zones Ia and Ib. Zone Ia: *Grindellia Stricta* fossils indicated a Ia zone. Other indicators: Low foraminifera count. *Trochammina macrescens* dominant species. Well-developed peat bed: Organic material makes up more than 2/3 of the sediment. Zone Ib: Foraminiferal assemblage zone with *Trochammina macrescens* and *Trochammina inflata*. Plant fossils dominated by *Spartina*. Muddy-peat to peaty-mud beds: Organic material makes up less than 2/3 of the sediment. Zone II: Foraminiferal assemblage zone with *Trochammina inflate (Ti)*, *Milliammina fusca (Mf)*, *Haplophragmoides manilaensis (Hm)*, and *Trochammina macrescens (Tmvm)*. Presence of *Milliammina fusca* indicates zone II. Sediments are composed of peaty mud and mud. Occasional plant rhizomes (Triglochin) in mud indicates zone II. Zone III: Foraminiferal assemblage zone dominated by *Milliammina fusca (Mf)*, with *Trochammina inflata* (Ti) and *Haplophragmoides manilaensis (Hm),* and lacking *Trochammina macrescens*. Sediments are composed of mud. Zone IV: Calcareous species present. Tidal heights: mean high high water (MHHW), mean high water (MHW), mean low high water (MLHW), and mean tide level (MTL).

deduced. Our results, in addition to previous studies, indicate that three or four foraminiferal assemblage zones are present in Humboldt Bay (Fig. 3; Shivelle *et al.*, 1991; Scott *et al.*, 1996). *Trochammina macrescens* dominated the composition in the upper reaches of the marsh; *Milliammina fusca* dominated the composition in the lower reaches. Both species occur in the transitional zone (Fig. 3). Although our elevation ranges for some of the foraminifera differ from some studies (e.g., Scott *et al.*, 1996), the patterns found within Humboldt

Bay are consistent with those found by other studies to the north in Oregon (i.e., Scott and Medioli, 1986; Jennings and Nelson, 1992; Hawkes *et al.*, 2010). Another identifier of the highest high marsh foraminiferal assemblage zone is a low total foraminifera count.

Methods

Lithology, macrofossils, and foraminiferal assemblages were used to identify RSL changes in the stratigraphy (Fig. 3). Lithology was the key means for identifying changes in the depositional environment, which was used as a primary tool to estimate the RSL from a stratigraphic bed. Various facies were identified based on texture, structure, and organic content. In order to assess the facies, this study mainly relied on the amount of organic material, which forms peat layers, in the sediment. In tidal channel exposures, these peaty beds were more resistant to erosion and formed steps in the banks of the channels. The highest environment, wetlands and forest, includes freshwater peat layers or forest litter layers without a significant amount of sediment.

Radiocarbon (^{14}C) dating provided age control (Ⓔ available in the electronic supplement to this paper). In most cases, material from several different plant species were combined to create a bulk date in order to collect enough material for conventional ^{14}C dating methods. We analyzed 55 original bulk peat samples and nine single-species plant samples (Vick, 1988; Valentine, 1992). The 57 bulk age determinations (55 samples with two split samples) were obtained using standard ^{14}C dating methods, which require 9 grams of material for analysis. The nine single-species samples were analyzed at the Center for Accelerator Mass Spectrometry (CAMS) using accelerator mass spectrometry (AMS) ^{14}C dating methods. The material was washed with deionized water, and the plant fragments were examined under a binocular microscope to remove roots intruding into the plant fragments. The ^{14}C ages were calibrated using the software program Calib 6.0 (Reimer *et al.*, 2009).

Reevaluation of Old Assumptions and Data

As much of this data was collected two to three decades ago, many studies have added to our understanding of the CSZ and paleoseismology utilizing marsh and estuarine stratigraphies. Thus, many new insights and methods have been added to this type of work since our original experimental plans were formulated. One important insightful advance in paleoseismicity has been the recognition that not all earthquakes may be recorded within the stratigraphy of estuaries. This concept, sometimes referred to as the magnitude threshold formation (McCalpin and Nelson, 1996) or evidence threshold (Nelson *et al.*, 2006), builds upon the recognition that many other factors come into play when determining the preservation potential of earthquake records such as flooded estuarine peats. Causes of this unequal preservation include the ability of crustal faults to accommodate fault movement, local sedimentation rates, bioturbation, the formation of local diastems, unequal ground shaking, and the cross-shelf distance from the epicenter of the subduction-zone earthquake. Some records are limited by the details of the site (McCalpin and Nelson, 1996). Taking these factors into account suggests that our record may represent the minimum number of earthquakes that occurred in northern California.

In addition to these advances in our understanding of the principles of paleoseismology, important advances have been made in geochronology. The most important advance is the ability to obtain radiocarbon ages from increasingly smaller amounts of material using AMS, thus improving the accuracy and precision in obtaining chronological constraints and in most modern studies avoiding the use of bulk peat dates. Ideally, dendrochronology would be used to correlate between sites, but fossil stumps were only found at two locations.

Although we sampled both plant fossils entombed in the overlying mud and bulk samples of peaty muds, most of our ages were obtained from bulk samples. A single entombed plant fossil best represents the age of the stratigraphic contact because the carbon accumulated in a short period of time, perhaps one to ten years, and the plant fossil was probably entombed by the event that caused the stratigraphic change. Bulk peat samples are problematic because they represent an accumulation of material that formed over tens of years and it is more difficult to rule out the possibility of contamination by roots from overlying stratigraphic units. While it is difficult to assess the errors associated with bulk samples, the duplicate bulk samples produced statistically similar ages. But given the uncertainties of bulk ages, the analytical errors must be taken as the minimum error associated with the ages.

Other advances have been made to obtain better constraints on the amount of RSL change using methods such as foraminifera and diatom transfer functions (e.g., Nelson *et al.*, 2008; Hawkes *et al.*, 2010, 2011). Often, using facies analysis alone, it may not be possible to distinguish the difference between low marsh and high marsh environments (Nelson, 1992). Although we found no significant lithologic difference that allows for discrimination between some environments such as low mudflat and high mudflat, we do feel confident in our ability to distinguish among the three marsh zones based on foraminifera and flora in most cases.

Late Holocene Stratigraphy of the Southern End of the Cascadia Subduction Zone (CSZ)

The following study sites are discussed from north to south. Vick (1988) first investigated the Mad River slough region, and Valentine (1992) conducted studies within Humboldt Bay. Li (1992) conducted studies on the Eel River delta. The foraminiferal assemblage zones for Humboldt Bay and the Eel River delta were evaluated by Manhart (1992) and Li (1992), respectively. For reference, the RSL zones (Ia, Ib, II, and III) from Figure 3 are used when discussing the RSL changes.

Mad River Slough

The Mad River slough lies within the northern limb of the Freshwater syncline (Fig. 2). This wetland formed in the lowlands behind the Mad River dunes. Meander scars indicate that the Mad River did not use the Mad River slough as a channel (Vick, 1988). Due to its proximity to the coastline, the stratigraphic record of the slough may be biased and influenced by changes in the configuration of the barrier island and estuary. Thus, the stratigraphic changes may also reflect circulation and tidal amplitude changes due to a reconfiguration of the Humboldt Bay system. However, when taken together with other records across northern California, local autogenic changes such as these can generally be ruled out. The Mad River slough has 5 km of readily accessible tidal exposures, which were investigated using lithologic, macrofossil, and foraminiferal stratigraphy.

General Stratigraphy. The Mad River slough contains evidence for five buried peat beds (Fig. 4). Along the tidal channel walls, the organic-rich peat beds are more resistant to erosion and form prominent benches. At its southern extent, the uppermost peat bed contains evidence for a transitional marsh to high marsh environment. The uppermost peat bed is nearly continuous to the northern extent of the slough, where stumps are rooted on top of the peat bed, indicating a woodland environment. A gap in the stratigraphy roughly correlates to the Fickle Hill anticline. The lowest peat beds are found only in the southern portion of the slough, are only exposed during spring low tides, and cannot be easily traced

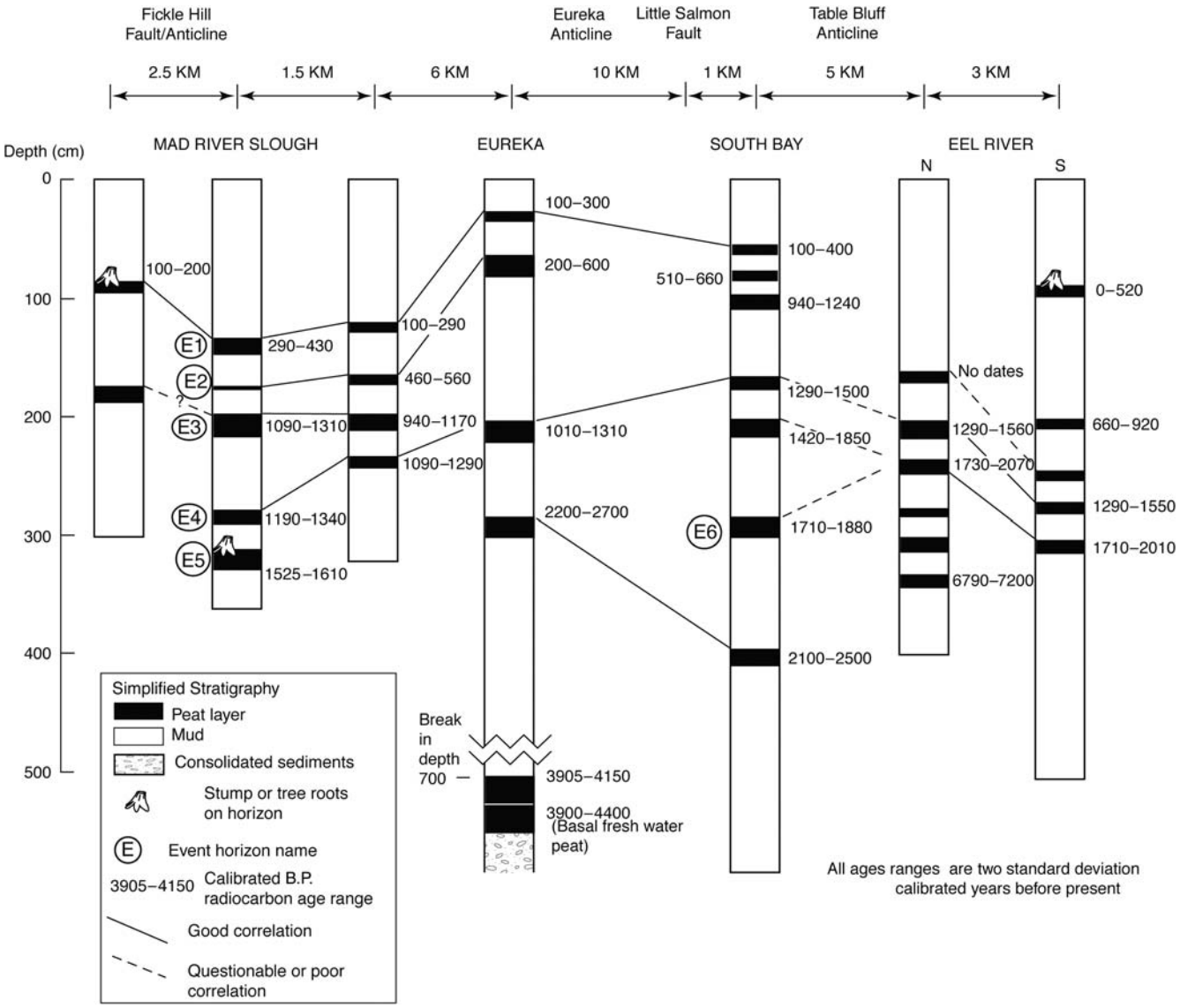

Figure 4. Correlation of the peat beds by radiocarbon age. Sites are shown from north to south. Simplified stratigraphic columns are composite columns for each area. All ages are calibrated radiocarbon years before present (cal B.P.). Supporting data for the interpretation of submergence events (labeled E1, E2, etc.) are summarized in Tables 1–6 and discussed in the text.

between sites. These lowest peat beds are correlated based on stratigraphic position and ^{14}C ages at two sites (CAMS 19,276, 1340 ± 50 radiocarbon years before present [RCYBP]; CAMS 19,120, 1270 ± 60 RCYBP).

Middle Mad River Slough Core 3 (MRS-3; Fig. 5). MRS-3 is on the outer bend of a large channel of the Mad River slough. The site contains five peat beds, four of which have ^{14}C dates. The lowest peat bed (305 cm) can be followed for

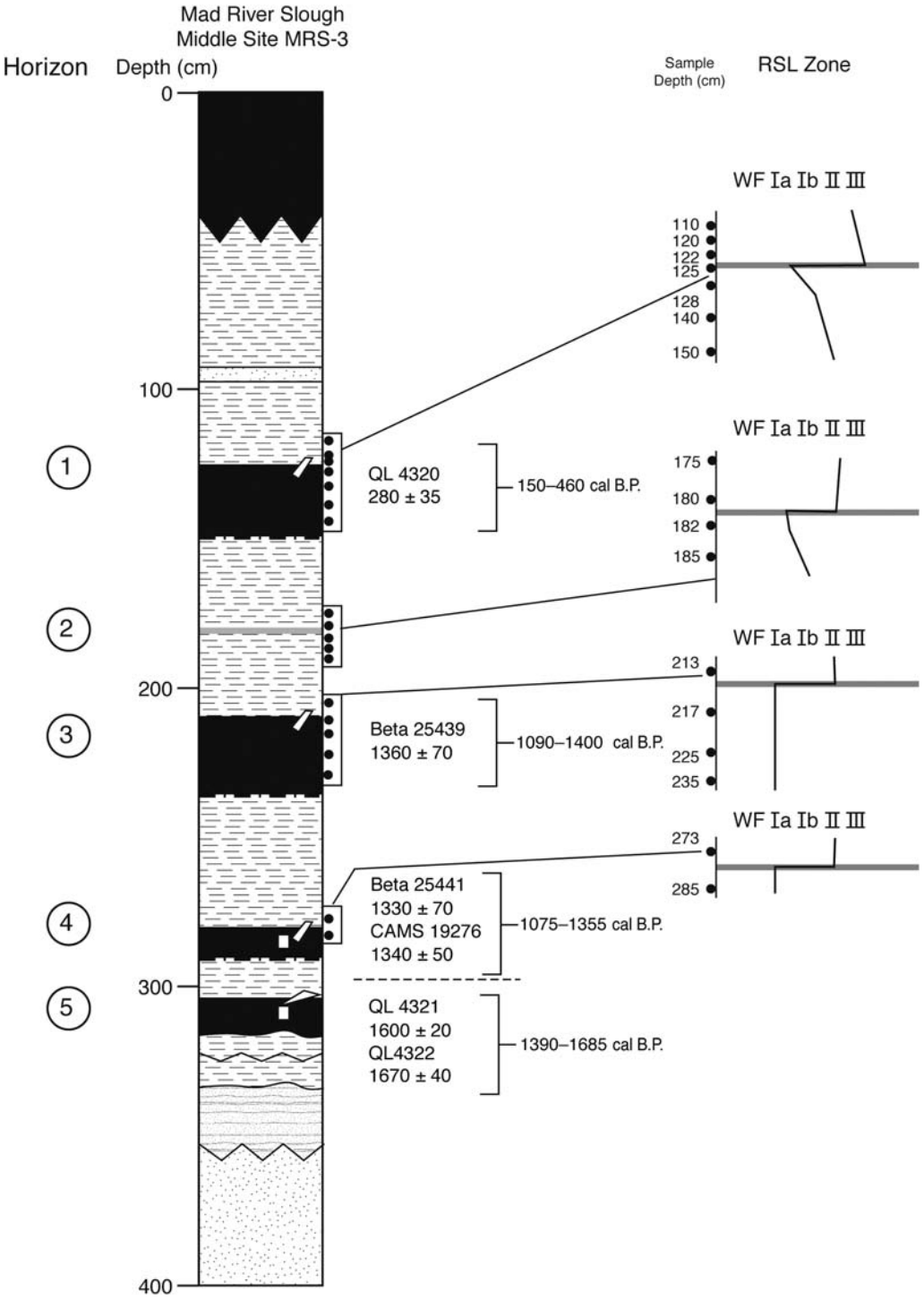

Figure 5. Lithological log of Mad River slough tidal channel exposure MRS-3. Five buried peat beds were identified. The third bed was initially identified by foraminiferal stratigraphy and was subsequently identified in the field as a thin peaty-mud bed. The lowest peat bed contains woody roots on the surface. All beds are interpreted as RSL increases across the peat–mud contact. Location is shown in Figure 2. Key applies to Figures 5–8.

over 100 m and contains fossils of woody roots. No stumps have been found on the lowest peat bed, but the presence of tree roots indicates that the lowest peat bed at this locality was inundated by saltwater no more than a couple of times a year. Three of the four upper peat beds (1, 3, and 4) contain entombed stems of *Grindelia stricta* extending into the overlying mud, indicating elevations near mean higher high water (MHHW). Fossils of *Distichlis spicata* protrude into the overlying layer and form an organic stratigraphic unit about 1–2 cm above the peat surface. The stems are bent over, which suggests drowning, sedimentation, bending, and subsequent burial.

The foraminiferal stratigraphy indicates submergence at each peat–mud contact (Fig. 5), but the changes are not of the same magnitude at each contact. Peat bed 3 and 4 foraminiferal assemblages and macrofossils indicate a high marsh environment (Ia). Peat bed 1 foraminiferal assemblage and macrofossils indicate that it was probably a high marsh environment (Ia). Peat bed 2 foraminiferal assemblage indicates a high/transitional marsh environment (I; Shivelle *et al.*, 1991).

The foraminiferal assemblages overlying the peat bed 3 and 4 contacts indicate a low marsh or mudflat zone (II/III), which suggests an RSL increase of 25–75 cm (Ia to II/III). The foraminiferal assemblage above peat bed 1 indicates a low marsh or mudflat environment (II/III), suggesting an RSL increase of between 25 and 75 cm (Ia to II/III). For peat bed 2, the change is to a marsh or mud flat (II/III), indicating around 25–50 cm of RSL change. The ^{14}C ages of peat beds 3 and 4 are nearly identical, yet there are 75 cm of sediment between the peat beds. This suggests two closely spaced submergence events (Fig. 5).

Lower Mad River Slough (MRS-6; Fig. 6). MRS-6 is the southernmost site in the Mad River slough. The site has four peat beds, all of which have ^{14}C dates. The slopes of the channel are steep. The beds can be followed for over 100 m. The foraminiferal assemblages and macrofossils from peat beds 1 and 2 indicate a high marsh environment (Ia). Both beds show a change in environment indicating submergence of the bed. The foraminiferal assemblage from above the contact on peat bed 1 changes to a transitional marsh environment (Ib), indicating an RSL increase of 0–25 cm (Ia to Ib). The foraminiferal assemblage from above the contact on peat bed 2 changes to a low marsh environment (II), indicating an RSL increase of between 25 and 75 cm (Ia to II). The ^{14}C ages indicate that the peat beds formed sometime after 1200 cal B.P. Similar to the lower Mad River slough, the radiocarbon ages from peat beds 3 and 4 are also closely spaced in time.

Eureka

The Eureka locations are on the southern limb of the Freshwater syncline (Fig. 2). Many of the examined areas are pocket marshes where marshes have filled small stream valleys in a region containing marine terraces. Unlike the Mad River slough study area, the surfaces are discontinuous, making it difficult to correlate between sites. Field examinations in the tidal channels along highly sinuous meanders in the other pocket marshes provide evidence that the present tidal channels and streams are eroding the stratigraphy in the Eureka area.

The sample sites with the best stratigraphy (Fig. 4) in the Eureka area are the marsh islands within Humboldt Bay and the pocket marshes within the in-filled stream valleys. The pocket marshes are adjacent to marine terraces. During the late 1800s and early 1900s, the Eureka region was the site of many sawmills and associated log storage facilities, which may have altered the stratigraphy in the tidal and stream channels, and left logging debris in the channels.

General Stratigraphy. The upper peat–mud contact is discontinuous and not present in all marshes. When exposed along the highway drainage channel, preserved channels cutting into the upper bed provide evidence that the meandering tidal channels and streams are altering the stratigraphy and removing evidence of the buried peat beds. With the exception of the upper two peat beds, where enough evidence is preserved, it is difficult to demonstrate any stratigraphic correlation between the pocket marshes. Radiocarbon ages suggest that deposits found within the cores are generally older than deposits from headwalls along Mad River slough. The absence of a continuous record of the recent stratigraphy is probably due to meandering channels removing and depositing sediment. The upper peat–mud contact correlates in age with the youngest peat bed at Mad River slough. Exposures in a highway drainage channel can be followed for over 100 m. Hand cores bottom out in a basal freshwater peat bed (QL4446, 3800 ± 60 RCYBP; Ⓔ see the electronic supplement to this paper) overlain by a tidal marsh peat bed.

Southern Humbolt Bay

Southern Humboldt Bay, or South Bay, is a syncline informally named South Bay syncline. Southern Humbolt Bay is on the lower plate of the Little Salmon fault and is bounded to the south by the Table Bluff anticline (Fig. 2). Ranchers periodically flooded the area causing an accumulation of sediment on the modern surface. Up to 75 cm of sediment has accumulated over the historic marsh surface in areas.

General Stratigraphy. The upper peat bed is found throughout the eastern portion of southern Humboldt Bay and can be followed in drainage channel exposures. Older peat beds in channel exposures are not continuous throughout southern Humboldt Bay, probably due to the migration of Little Salmon Creek between three channel mouths. Thus, the stratigraphic record of submergence events may be incomplete. However, some lower peat beds were traced in a vibracore transect (Fig. 4).

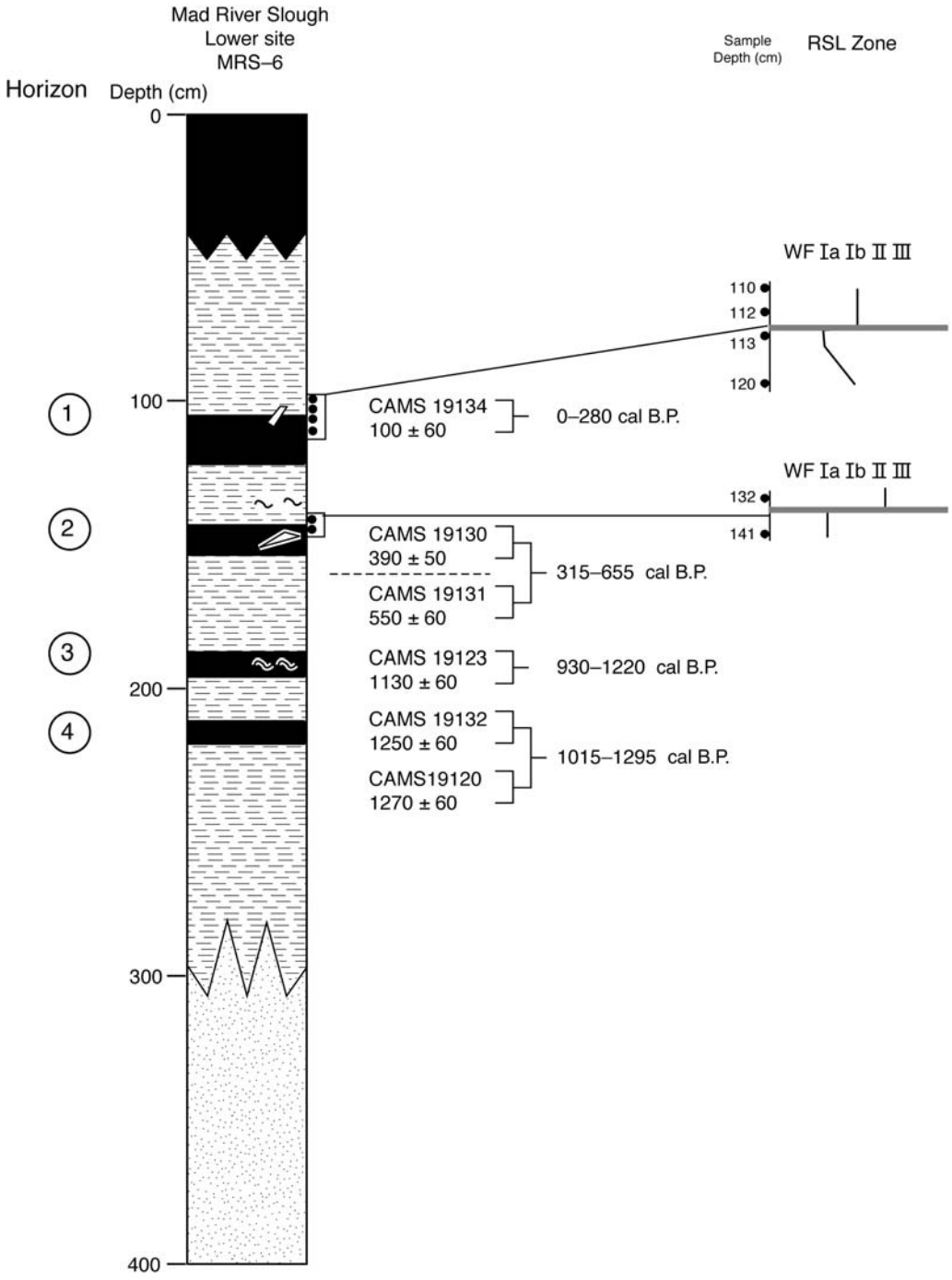

Figure 6. Lithological log of Mad River slough tidal exposure MRS-6. Four beds were identified at this location. The first two beds have foraminiferal assemblages indicating RSL increases, although the contact across the top of the first peat bed may not be significant. Radiocarbon ages back to 1290 cal B.P. represent the four most recent submergence events. Location is shown in Figure 2.

Vibracore 15 (VC15; Fig. 7). VC15 sampled four organic-rich beds with varying thicknesses and characteristics (Fig. 7). The first two peat beds are thin. The uppermost has an irregular contact. Peat bed 2 is interpreted as a high marsh environment (Ia) due to its high organic content. Peat bed 3 has a thin (< 2 cm) cap of peaty mud. The foraminiferal stratigraphy and macrofossils document the emergence of the third sequence (underlying mud to peat bed 3 to overlying mud) from a tidal mudflat (III) to a high marsh environment (Ia) and back to a low marsh environment (II) across the bed 3 contacts. The sequence begins with a gradual RSL decrease that represents the accumulation of sediment to a high marsh environment (Ia). Across bed 3, the foraminiferal assemblage changes to a low marsh environment (II), supporting an RSL increase of 25–50 cm in depth. The lowest peat bed, bed 4, is a strong peat that has a clear contact with the overlying mud.

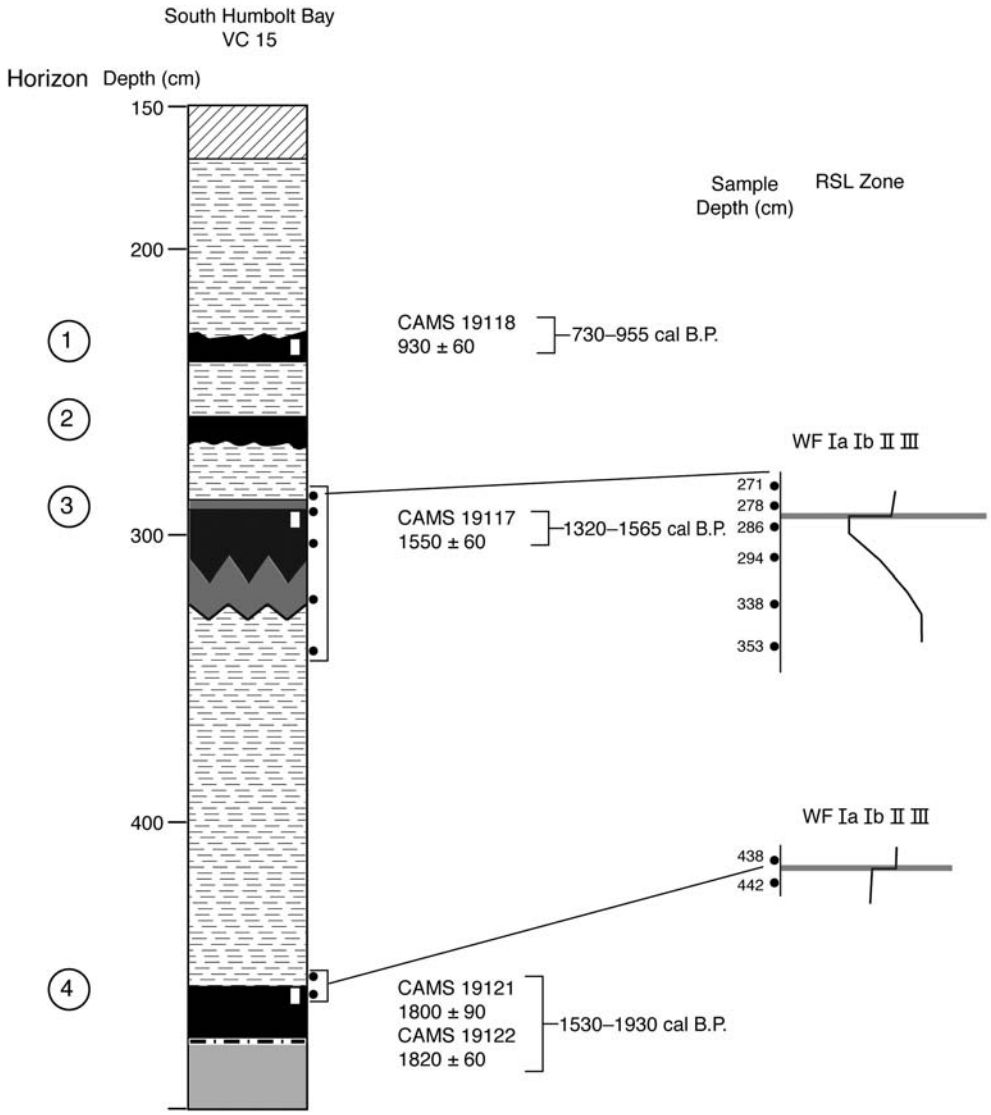

Figure 7. Lithological log for South Humbolt Bay vibracore VC-15. Four peat beds were identified with the two lowest beds showing RSL changes at their upper contacts (the two upper beds do not have foraminiferal data). A radiocarbon age on the third peat bed was lost during processing. Location is shown in Figure 2. (Note: Core log starts at 150 cm.)

Foraminiferal assemblages show a small change across the contact from a high/transitional marsh (I) to a low marsh (II) zone (0–25 cm).

Eel River Delta

The Eel River delta region is a large broad expanse of floodplain south of the Table Bluff anticline and north of the Cape Mendocino marine terraces. Li (1992) conducted three vibracore transects in the north and south portions of the Eel River delta (Fig. 2). The region contains evidence for up to seven stratigraphically distinct peat beds.

General Stratigraphy. The northern Eel River vibracore transects (Fig. 4) contain seven difficult-to-correlate organic-rich beds with ages up to 6690 ± 100 RCYBP (Ⓔ see BETA 4990 in the electronic supplement to this paper; Fig. 4). Many of the beds lack clear contacts, and the beds are thin and discontinuous. The stratigraphy contains ambiguous RSL information because many of the foraminiferal assemblages indicate either no zone change or one environmental zone change between beds.

The southern Eel River transect (Eel Transect C, Fig. 4) is located in a back dune region similar to the Mad River slough. The site contains five peat beds. The foraminiferal stratigraphy provides good evidence of coseismic subsidence across the stratigraphic boundaries.

Southern Eel River Vibracore Transect Core 6 (ER-VC-06; Fig. 8). The buried peat beds at this site are thicker and easier to trace than those at the northern Eel River transects. Peat bed 2 foraminiferal assemblages indicate an RSL rise from high marsh (Ia) to transitional/low marsh (Ib/II), an RSL rise of 0–50 cm. Bed 3 foraminiferal assemblages indicate an

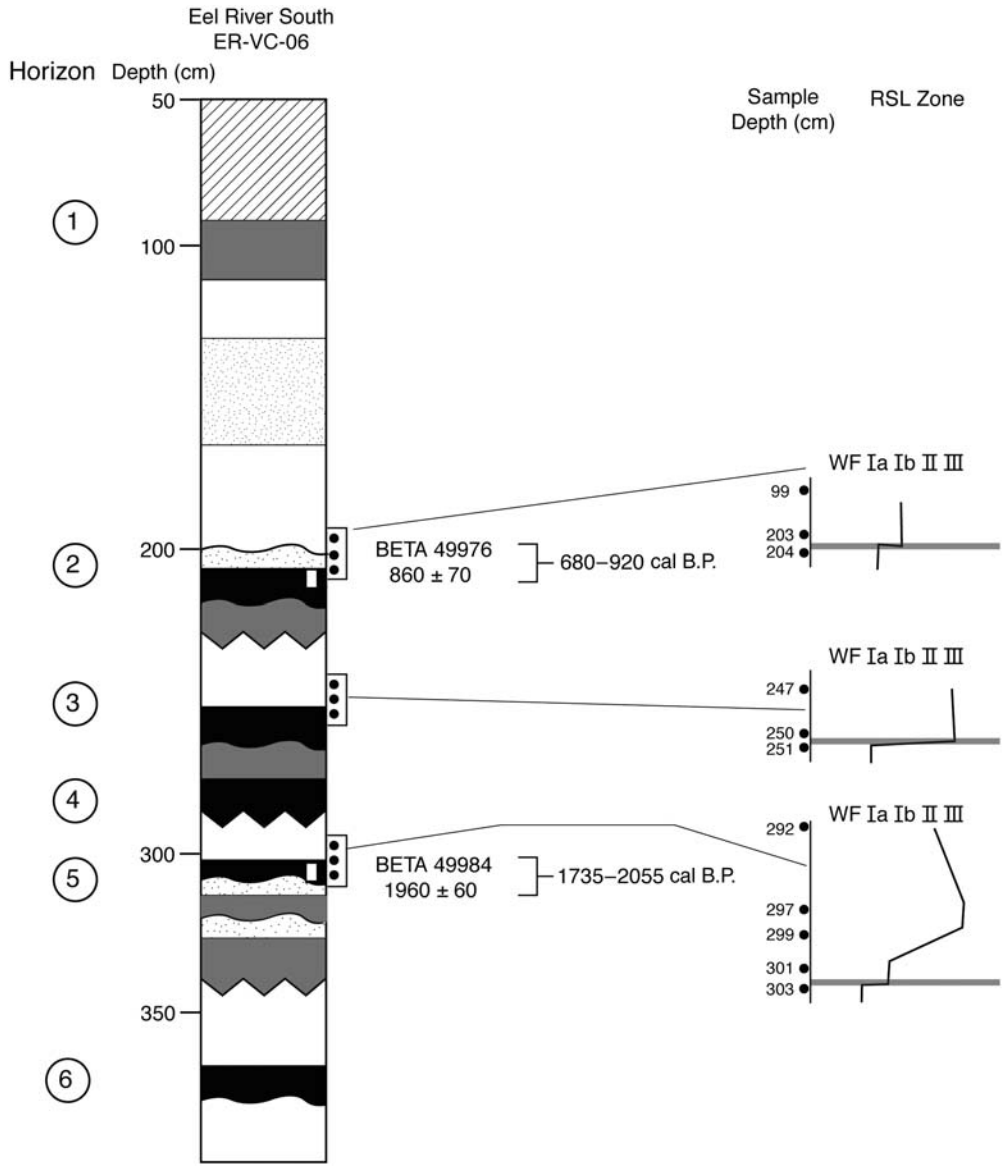

Figure 8. Lithological log for Eel River vibracore ER-VC-06. Six peat beds were identified with two beds containing evidence for a significant RSL increase (submergence) at the upper contact. Undated bed 3 (250 cm) shows a drop of over 75 cm. Bed 5 (300 cm) shows a rapid increase in RSL of 50–75 cm over 4 cm of sediment. Location is shown in Figure 2. (Note: Core log starts at 50 cm. Modified from Li, 1992.)

RSL rise from high marsh (Ia) to mudflat (III) zone, an RSL rise (submergence) of >75 cm. There is no mud contact between beds 3 and 4. Based on the lithology, bed 4 marks the transition from a high/transitional marsh to a low marsh. Bed 5 foraminiferal assemblages indicate an RSL rise from high/transitional marsh (I) to mudflat (III) zone, although the transition is not found exactly at the contact. This represents an RSL increase (submergence) of 25–50 cm.

Possible Record of Past Earthquakes

Potential Magnitude of Past Earthquakes

There are many potential problems with assessing the extent of rupture for past earthquakes. The accuracy of the dating techniques presents the largest problem. Nelson *et al.* (2006) discuss the difficulties of using ^{14}C ages to correlate past earthquakes between regional sites, and provide criteria for identifying regional subsidence due to large earthquakes. The potential magnitude of earthquakes ranges from a great entire subduction zone breaking M_w 9.1 (Verdonk, 1995), to a smaller single to multiple segment breaking M_w 8.2–8.4 (Verdonk, 1995), to smaller earthquakes on local faults with magnitudes of approximately M_w 6.5–7.2. Data may indicate that earthquakes from different localities were closely spaced in time and that they affected large regions, but it is not possible to state that the earthquakes at different localities are identical in time. Historic examples for the large single earthquake breaking multiple segments are the 1960 Chile earthquake (M_w 9.5) and the 2004 Great Sumatra–Andaman earthquake (M_w 9.1). A historic example for a

subduction zone breaking single segments during different earthquakes closely spaced in time is the Nankaido subduction zone in Japan (1946 and 1947 with magnitudes of M_w 7.4 and 7.2, respectively). Scenarios could include the entire CSZ rupturing in a great earthquake and the CSZ rupturing in segments as a series of major earthquakes.

Current models of characteristic earthquakes and segmentation for subduction zones may not be applicable. Although the Chilean subduction zone ruptured as one big earthquake, it may have also previously ruptured as several smaller earthquakes. Muir-Wood (1989) documents evidence that the 1857 rupture affected the southern portion of the 1960 Chilean earthquake deformation zone, and that the 1960 Chilean earthquake ruptured across several segment boundaries. In addition, the 2010 Chilean earthquake ruptured a 500-km segment of the subduction zone (Vigny *et al.*, 2011) north of the 960-km long 1960 rupture (Cifuentes, 1989). These two earthquakes were only 40 years apart, which is indistinguishable by ^{14}C dating. This leads to the question of how to estimate paleoseismic magnitude for subduction zones. Are they treated as a single unit or as segments?

This study uses the patterns of evidence for coseismic subsidence to evaluate the possible magnitudes of earthquakes. The potential magnitude is evaluated based on differences in the zones of subsidence and the magnitude of subsidence for a local earthquake compared to an earthquake rupture along an entire subduction zone. A regional or entire zone rupture should cause coseismic subsidence at all sites in the southern end of the CSZ and at many sites along the Pacific Northwest coast. A local earthquake on the Little Salmon fault may only cause subsidence in the southern Humboldt Bay and the Freshwater syncline (Mad River slough and Eureka), while showing no evidence of subsidence in the Eel River delta.

Great Earthquake. The maximum extent of rupture is a great earthquake encompassing the entire length of the subduction zone, about 1200 km, similar to the rupture length of the 2004 Great Sumatra–Andaman earthquake (Ammon *et al.*, 2005). The estimated magnitude for an entire subduction-zone event would be approximately M_w 9.0 (Verdonk, 1995; Leonard *et al.*, 2010). Evidence for a great prehistoric subduction earthquake ($M_w > 9.0$) would be found at sites along the Pacific Northwest coast. Unfortunately, radiocarbon precision does not allow for precise correlation of sites. Submergence evidence can only be used to infer the possibility of an earthquake. Using other evidence such as tsunami sand beds and turbidites along the southern CSZ, it has been argued that many $M_w > 9.0$ subduction-zone earthquakes have occurred (Carver *et al.*, 1999; Kelsey *et al.*, 2002, 2005; Goldfinger *et al.*, 2003). This does not exclude the possibility of smaller earthquakes.

Regional Earthquake of the Southern CSZ. Matching the present day geodetic information with 3D deformation models suggests that earthquakes of magnitude $M_w > 8.3$ could occur for ruptures encompassing the southern half of the subduction zone (Verdonk, 1995; Leonard *et al.*, 2010). Using the empirical relationships from Wells and Coppersmith (1994), the magnitude of the southern quarter of the subduction zone rupturing would be M_w 8.2 for a rupture of width 240 km long by 80 km wide, with an estimated slip of 8 m (Toppozada *et al.*, 1995). The expected effects of such an earthquake are subsidence at all of the coastal sites and possible coseismic slip on the Little Salmon and McKinleyville faults.

Local Earthquake. Several fault zones, such as the Little Salmon and Mad River fault zones, traverse the northern California region. If they produce large earthquakes independently of the CSZ, then local earthquakes on individual faults in the fold and thrust belt increase the seismic hazard for the southern end of the CSZ. Using the empirical relationships of Wells and Coppersmith (1994), the Little Salmon fault is capable of a M_w 6.5–7.2 earthquake assuming a rupture length of 20–60 km and a width of 12–20 km.

The expected effects of such an earthquake are minor amounts of subsidence within the frontal syncline adjacent to the fault, larger amounts of subsidence in the syncline behind the fault, or uplift. For an earthquake on the Little Salmon fault, subsidence would be expected in southern Humboldt Bay and the Freshwater syncline (Mad River slough) but not in the Eel River delta. For an event on the Mad River fault zone, subsidence would be expected in the Freshwater syncline (Mad River slough) but not in southern Humboldt Bay or the Eel River delta. Subsidence would be variable from 0.25–1 m in the frontal portion to 1–3 m in the back basin.

Proposed Earthquakes

Using the ^{14}C age control and the submergence history, there are six possible earthquakes (Tables 1–7 and Fig. 9). As other environmental changes such as a rapid increase in eustatic sea-level rise (such as that documented by Cronin *et al.* (2007) for the 8.2 ka climate anomaly) or changes in tide levels caused by reorganizations of the bay (as suggested by Nelson *et al.*, 2008) can cause flooding recorded in wetland stratigraphy, we refer to each of our periods of rapid sea-level rise as submergence events. The true test of whether the submergence events are coseismically derived or the result of eustatic sea-level jumps lies in the concurrent record of tsunamis or shaking records (e.g., liquefaction, landslides, earthquake-triggered turbidites, etc.). While there is evidence for six submergence events in the region, only the middle Mad River slough site contains a nearly complete stratigraphic record of the possible earthquakes (it lacks rapid submergence event E6). However, the stratigraphy site correlation (Fig. 4) may not be accurate, because beds cannot be traced from syncline to syncline. Furthermore, the errors in and the range of the correlated ^{14}C ages limit its use to directly correlate sites. Submergence events with a question

Table 1
Summary of Ages of and Evidence for Submergence Event E1*

Ages (cal B.P.)	Sites	RSL (Zones)	Comments
90–290; 280–500; 0–280	Mad River slough	0–75 cm (Ia/b–III, Ia–Ib)	Woodland soils with stumps and peat horizons with *Grindelia* stems overlain by estuarine mud.
280–426	Eureka		Peat overlain by estuarine mud.
0–280	Southern Humbolt Bay		Peat overlain by modern surface.
0–460	Eel River delta		Stumps overlain by mud and then sand. Not correlative with stumps in Mad River slough.

Other recently published records with earthquake proxies of a similar age: Willapa Bay, Washington; Copalis River, Washington; Grays Harbor, Washington; Columbia River, Washington (Atwater *et al.*, 2004); Greyland Plains, Washington; Willapa Bay, Washington; Rockaway, Oregon; Neskowin, Oregon (Schlichting and Peterson, 2006); Netarts Bay, Oregon (Darienzo and Peterson, 1990); Alsea Bay, Oregon; Coos Bay, Oregon (Nelson *et al.*, 2008); Coquille River, Oregon (Witter *et al.*, 2003); Bradley Lake, Oregon (Kelsey *et al.*, 2005); Sixes River, Oregon (Kelsey *et al.*, 2002); Nestucca River, Oregon (Hawkes *et al.*, 2010); offshore turbidites (Adams, 1990; Goldfinger *et al.*, 2003).

Interpretation: Occurred between 230–270 cal B.P. Represents an entire CSZ rupture corresponding to the 26 January 1700 CSZ earthquake.

*Summary of the evidence for submergence event E1 along the northern California coast and the interpreted magnitude of the earthquake (local versus regional). Blanks indicate no evidence of an earthquake at that location during that time interval. If the region is unlisted, that indicates the absence of sediment from that time period. See Figure 1 for the location of other earthquake proxies.

Table 2
Summary of Ages of and Evidence for Submergence Event E2(?)*

Ages (cal B.P.)	Sites	RSL (Zones)	Comments
315–655	Mad River slough	0–50 cm (Ia–II, Ib–II)	Peat horizon overlain by mud. Thin in locations. Not present in the upper reaches.
440–660	Eureka		Peat overlain by mud. Found on bay islands.
550–680	Southern Humbolt Bay		Peat overlain by mud overlain by modern surface in tidal channel exposure.
680–920	Eel River delta		Peat overlain by mud overlain by undated layer. Note: age older than other sites.

Other recently published records with earthquake proxies of a similar age: Greyland Plains, Washington; Willapa Bay, Washington (700 cal B.P.; Schlichting and Peterson, 2006); Alsea Bay, Oregon (800 cal B.P.; Nelson *et al.*, 2008); offshore turbidites (Adams, 1990; Goldfinger *et al.*, 2003).

Interpretation: Occurred between 500–600 cal B.P. Evidence for an earthquake is tentative. May represent local earthquake or RSL change from other cause.

*Summary of the evidence for submergence event E2(?) along the northern California coast and the interpreted magnitude of the earthquake (local versus regional). Blanks indicate no evidence for an earthquake at that location during that time interval. If the region is unlisted, that indicates the absence of sediment from that time period. See Figure 1 for the location of other earthquake proxies.

Table 3
Summary of Ages of and Evidence for Submergence Event E3*

Ages (cal B.P.)	Sites	RSL (Zones)	Comments
940–1264; 1175–1355	Mad River slough	25–50 cm (Ia–II)	Peat overlain by mud. Overlain by submergence event E2(?).
1090–1290; 1280–1500	Eureka		Unlike Mad River slough, there is no stratigraphic way to separate submergence events E3 and E4. Also listed as submergence event E4.
730–955; 710–950	Southern Humbolt Bay	0–50 cm (I–II)	Peat overlain by mud, overlain by submergence event E2(?). Peat overlain by mud, overlain by undated bed in another core.
940–1240	Eel River delta	0–50 cm (I–II)	Peat overlain by sand (possible tsunami), then mud.

Other recently published records with earthquake proxies of a similar age: Greyland Plains, Washington; Willapa Bay, Washington (Schlichting and Peterson, 2006); Alsea Bay, Oregon (Nelson *et al.*, 2008); Coquille River, Oregon (Witter *et al.*, 2003); Bradley Lake, Oregon (Kelsey *et al.*, 2005); Sixes River, Oregon (Kelsey *et al.*, 2002); offshore turbidites (Adams, 1990; Goldfinger *et al.*, 2003).

Interpretation: Occurred between 1000–1250 cal B.P. Evidence for two earthquakes closely spaced (submergence events E3 and E4). Based on smaller amplitude changes and record of movement along the Little Salmon fault; this submergence event is interpreted to be a local earthquake and E4 to be a regional or entire CSZ earthquake.

*Summary of the evidence for submergence event E3 along the northern California coast and the interpreted magnitude of the earthquake (local versus regional). Blanks indicate no evidence for an earthquake at that location during that time interval. If the region is unlisted, that indicates the absence of sediment from that time period. See Figure 1 for the location of other earthquake proxies.

Table 4
Summary of Ages of and Evidence for Submergence Event E4*

Ages (cal B.P.)	Sites	RSL (Zones)	Comments
1015–1295; 1170–1345	Mad River slough	25–50 cm (Ia–II)	Peat overlain by mud with Triglochin rhizomes. Overlain by submergence event E3.
1090–1290; 1280–1500	Eureka		Unlike Mad River slough, there is no stratigraphic way to separate submergence events E3 and E4. Also listed as submergence event E4.
1170–1290; 1320–1565	Southern Humbolt Bay	> 50 cm (I–III)	Peat covered by thin muddy peat—entombed plants(?)—overlain by peat with basal age of 730-955 cal B.P.
960–1410	Eel River delta		Peat overlain by mud overlain by unlogged sediment.

Other recently published records with earthquake proxies of a similar age: Columbia River, Washington (Atwater *et al.*, 2004), Greyland Plains, Washington; Willapa Bay, Washington; Neskowin, Oregon (Schlichting and Peterson, 2006); Netarts Bay, Oregon (Darienzo and Peterson, 1990); Alsea Bay, Oregon (Nelson *et al.*, 2008); Coquille River, Oregon (Witter *et al.*, 2003); Bradley Lake, Oregon (Kelsey *et al.*, 2005); Sixes River, Oregon (Kelsey *et al.*, 2002); offshore turbidites (Adams, 1990; Goldfinger *et al.*, 2003).

Interpretation: Occurred between 1150–1400 cal B.P. Evidence for two earthquakes closely spaced (submergence events E3 and E4). Based on larger amplitude changes,this submergence event is interpreted to be a regional or entire CSZ earthquake.

*Summary of the evidence for submergence event E4 along the northern California coast and the interpreted magnitude of the earthquake (local versus regional). Blanks indicate no evidence for an earthquake at that location during that time interval. If the region is unlisted that indicates the absence of sediment from that time period. See Figure 1 for the location of other earthquake proxies.

Table 5
Summary of Ages of and Evidence for Submergence Event E5(?)*

Ages (cal B.P.)	Sites	RSL (Zones)	Comments
1390–1565	Mad River slough		From tidal exposure overlain by surface dated at 1015–1295 cal B.P. Horizon contains roots but no stumps.
1520–1810	Southern Humbolt Bay	−25 cm (fall) to 50 cm (Ib–Ia, Ia–II)	Ambiguous foraminifera data from two different cores.
1350–1560	Eel River delta	> 75 cm (Ia–III)	Peat overlain by mud in southern Eel River transect. Succession overlain by undated thin peat layer. Date correlated from ER-VC-07.

Other recently published records with earthquake proxies of a similar age: Netarts Bay, Oregon (Darienzo and Peterson, 1990); Alsea Bay, Oregon (Nelson *et al.*, 2008); offshore turbidites (Goldfinger *et al.*, 2003).

Interpretation: Occurred between 1500–1650 cal B.P. Considering the unclear nature of the stratigraphy and only one other correlation site, this is possibly a local earthquake or caused by another mechanism.

*Summary of the evidence for submergence event E5(?) along the northern California coast and the interpreted magnitude of the earthquake (local versus regional). Blanks indicate no evidence for an earthquake at that location during that time interval. If the region is unlisted, that indicates the absence of sediment from that time period. See Figure 1 for the location of other earthquake proxies.

Table 6
Summary of Ages of and Evidence for Submergence Event E6*

Ages (cal B.P.)	Sites	RSL (Zones)	Comments
	Mad River slough		Record does not extend this far back in time.
1730–1880	Eureka		Peat overlain by mud and shell layer. Succession overlain by modern surface.
1710–1880; 1810–1990	Southern Humbolt Bay	0–50 cm (I–II)	Strong peat overlain by 1.5 m mud layer. Overlain by submergence event E5(?).
1730–2070 1735–2055	Eel River delta	> 50 cm	Peat and soil layers overlain by mud. Overlain by 3 other submergence events with the uppermost having an age of 680–920 cal B.P.

Other recently published records with earthquake proxies of a similar age: Willapa Bay, Washington; Copalis River, Washington; Columbia River, Washington (Atwater *et al.*, 2004); Netarts Bay, Oregon (Darienzo and Peterson, 1990); Alsea Bay, Oregon (Nelson *et al.*, 2008); Coquille River, Oregon (Witter *et al.*, 2003); Bradley Lake, Oregon (Kelsey *et al.*, 2005); Sixes River, Oregon (Kelsey *et al.*, 2002).

Interpretation: Occurred between 1750–1900 cal B.P. Possibly a regional or entire CSZ earthquake.

*Summary of the evidence for submergence event E6 along the northern California coast and the interpreted magnitude of the earthquake (local versus regional). Blanks indicate no evidence for an earthquake at that location during that time interval. If the region is unlisted, that indicates the absence of sediment from that time period. See Figure 1 for the location of other earthquake proxies.

Table 7
Summary of the Ages and Significance of Submergence Events*

Submergence Event	Age Range (cal B.P.)	Comments
E1	230–270	Regional earthquake. Possible correlation with entire subduction zone.
E2(?)	500–600	Questionable—local earthquake(?). Age ranges do not match at all sites, but Mad River slough has good evidence for submergence at two sites. Questionable regional correlation.
E3	1000–1250	Local earthquake. Good RSL change in Mad River slough; smaller in Eel River delta and South Bay. Possible correlation with movement along Little Salmon fault.
E4	1150–1400	Regional earthquake. All sites show good evidence for rapid submergence.
E5(?)	1500–1650	Questionable—(local earthquake(?). Good age correlation, but ambiguous RSL changes. Good evidence for submergence of trees into intertidal zone in Mad River slough.
E6	1750–1900	Possible regional earthquake. Good evidence for submergence. Possible correlation with event on Little Salmon fault.

*Summary of our interpreted record of paleo-earthquakes for the southern end of the CSZ. The calculation of a recurrence interval is not appropriate, because the earthquakes could have occurred on different faults.

mark following the letter—for example, E2(?)—are questionable (Tables 1–7). Such periods of rapid submergence lack strong evidence for coseismic subsidence, site to site correlation, or an extensive presence in the region.

Submergence Event E1 (230–270 cal B.P.; Entire Zone).

Evidence for Submergence Event E1. The youngest event, submergence event E1, is present at all sites and contains strong evidence for coseismic subsidence (Table 1 and

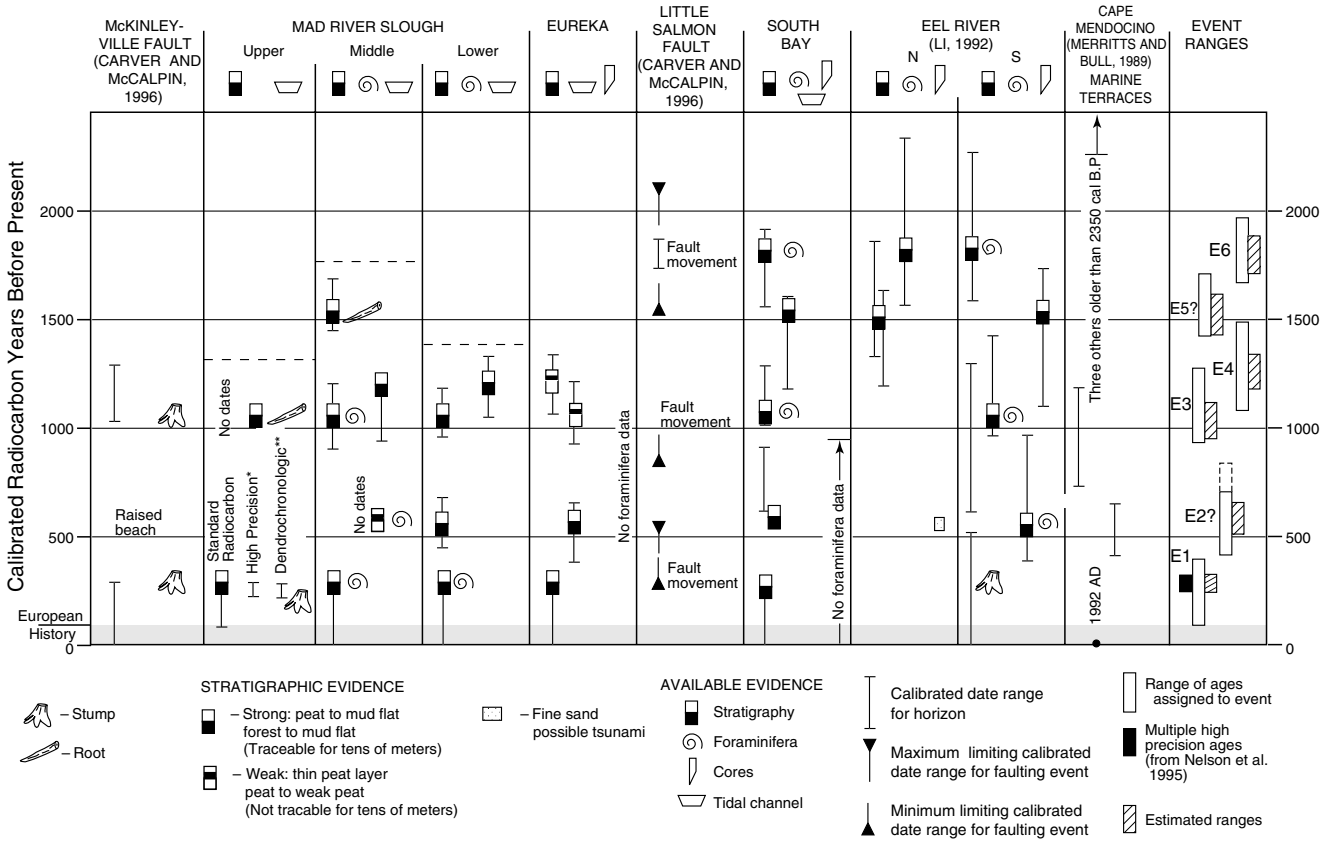

Figure 9. Summary of the evidence for past earthquakes from locations between the McKinleyville fault and Cape Mendocino. Based on the stratigraphy, we interpret six past earthquakes. Four of these paleoearthquakes are interpreted from fault trench studies and other paleoseismic sites (from Clarke and Carver, 1992; Carver and McCalpin, 1996). The most recent submergence event is marked by stumps and several other studies suggesting that it is was a large earthquake, possibly rupturing the entire subduction zone. High precision ages (denoted by *) in upper Mad River slough from Nelson *et al.* (1995). Dendrochronological age (denoted by **) in upper Mad River slough from Jacoby *et al.* (1995).

Fig. 9). At the upper end of the Mad River slough, rooted stumps are found on this bed representing the submergence event, and, in places, the mud overlying the peat bed contains *Triglochin martimium* fossils, a mudflat-pioneering marsh species. The foraminiferal assemblages from the Mad River slough show a rise in RSL (Ia–Ib and Ia–III; increasing water depth), which indicates between 0 and 75 cm of submergence. Evidence for submergence event E1 is also found on the Little Salmon fault (Carver and McCalpin, 1996). Using multiple ^{14}C ages, Nelson *et al.* (1995) dated this bed in the middle Mad River slough at around A.D. 1700.

Magnitude of Submergence Event E1. This study finds evidence for submergence event E1 at every northwestern California location (Table 1 and Fig. 9), and ^{14}C ages from stumps in the Mad River slough have similar ages to stumps found elsewhere along the CSZ (Nelson *et al.*, 1995). Several authors have found evidence of coseismic subsidence and postseismic uplift in the shallow estuaries of southwest Oregon and Washington that date to this time (Darienzo and Peterson, 1990; Kelsey *et al.*, 1998, 2002, 2005; Witter *et al.*, 2003; Atwater *et al.*, 2004; Nelson *et al.*, 2006, 2008; Hawkes *et al.*, 2010, 2011). In addition, Satake *et al.* (1996) associated a tsunami recorded in Japan on 23 January 1700 with the CSZ. Similar tsunami deposits have been found within coastal areas of Oregon as well (Kelsey *et al.*, 2002, 2005; Schlichting and Peterson, 2006). The offshore turbidite record also records an earthquake at this time (Goldfinger *et al.*, 2012). Based on this evidence, the hypothesis that the entire subduction zone ruptured in the most recent event has not been falsified.

Submergence Event E2(?) (500-600 cal B.P.; Questionable Regional).

Evidence for Submergence Event E2(?). Evidence for submergence event E2(?) is found at all four California locations (Table 2 and Fig. 9), although it is problematic that the stratigraphic signature of the submergence event can only be attributed to coseismic subsidence. At many sites, the bed lacks continuity and is a muddy-peat or peaty-mud bed rather than a true peat bed. At middle Mad River slough, evidence for the submergence event is a thin muddy-peat bed, which did not form the characteristic step like the other peat beds in tidal exposures. The foraminiferal assemblages from the middle Mad River slough site provide evidence of a significant RSL increase (submergence) from high marsh to low marsh (Ia–II; 25–50 cm). The foraminiferal assemblages at other sites show RSL increases, which support an increase in the water depth across the peat–mud contacts but that are not of significant magnitude to support coseismic subsidence.

Magnitude of Submergence Event E2(?). Questionable evidence for submergence event E2(?) is found at all locations (Table 2 and Fig. 9). The ages for the Eel River delta are older than the other sites. While this evidence indicates problems with the data supporting this submergence event, there are coseismically generated turbidities reported during this time period (Adams, 1990; Goldfinger *et al.*, 2003, 2012). In addition, the error bars overlap the age of tsunami deposits found in Willipa Bay and Greyland Plains, Washington (700 cal B.P.; Schlichting and Peterson, 2006), and Alsea Bay, Oregon (800 cal B.P.; Nelson *et al.*, 2008). However, Schlichting and Peterson (2006) suggest that this tsunami may have been sourced from a non-CSZ earthquake. Although these earthquake proxies could be coincidental changes at several sites that cannot be distinguished using the present age control, they could also indicate that this was a local earthquake (M_w 6.5–7.2), or if they produced the turbidite layer off southern Oregon and northwestern Washington, it could represent a regional earthquake ($M_w > 8.2$). However, a recent compilation of earthquakes from throughout the CSZ by Nelson *et al.* (2006) did not find evidence for a widespread earthquake 500–600 cal B.P. It also does not appear in the tsunami record from Bradley Lake, Oregon, which is thought to record all CSZ earthquakes (Kelsey *et al.*, 2005). There is not sufficient evidence from the data to evaluate the cause(s) of this RSL event or whether it represents a coseismic subsidence due to an earthquake or coincidental RSL changes at several sites. If an earthquake caused the observed RSL changes, then based on the distribution of the changes the earthquake was probably a local event.

Submergence Events E3 (1000–1250 cal B.P.; Local to Regional) and E4 (1150–1400 cal B.P.; Regional).

Evidence for Submergence Events E3 and E4. Submergence events E3 and E4, are closely spaced in time but are separated stratigraphically when both are present at the same site. Beds with ages in the range of 1000–1400 cal B.P. are found at all sites (Tables 3 and 4 and Fig. 9), and the ages cannot be differentiated easily unless beds representing both submergence events are preserved. Varying amounts of sediment separate the submergence event beds: 65 cm in the middle Mad River slough, 40 cm in the lower Mad River slough, and 150 cm in southern Humboldt Bay. In the Mad River slough, both peat–mud contacts show good evidence of submergence (Ia–II; 25–50 cm). In southern Humboldt Bay, foraminifera show good evidence for submergence (I–III; >50 cm) across submergence event E4. Similarly, in the Eel River delta, foraminifera show good evidence for submergence (I–II; 0–50 cm) across submergence event E3. There is one documented faulting event in this age range along the Little Salmon fault (Carver and McCalpin, 1996). The evidence supports two earthquakes large enough to submerge sites at the southern end of the CSZ within 300 years.

Magnitude of Submergence Events E3 and E4. A local earthquake followed by a CSZ earthquake best explains the stratigraphy and timing of submergence events E3 and E4. One of the faulting ruptures along the Little Salmon fault occurred within this time period (Clarke and Carver, 1992; Carver and McCalpin, 1996). Based on the estimated magnitude of submergence, the younger submergence event E3

was smaller than the older submergence event E4. This suggests that submergence event E3 was associated with movement on the Little Salmon fault and that the secondary thrusts in northern California are capable of independent movement producing earthquakes of magnitude M_w 6.5–7.2.

Evidence for a regional CSZ earthquake at about the same time has been found in the stratigraphy of at least seven other locations further north along the CSZ (Darienzo and Peterson, 1990; Nelson *et al.*, 1996, 2006, 2008; Shennan *et al.*, 1996, 1998; Witter *et al.*, 2003; Atwater *et al.*, 2004; Kelsey *et al.*, 2005) and within the offshore turbidite record (Goldfinger *et al.*, 2012). Although limited by our chronostratigraphic constraints, based on the recent summary by Nelson *et al.* (2006), submergence event E4 better fits a regional earthquake while submergence event E3 most likely represents a local earthquake.

Submergence Event E5(?) (1500–1650 cal B.P.; Questionable, Local).

Evidence for Submergence Event E5(?). Submergence event E5(?) is the oldest submergence event documented in the Mad River slough (Table 5 and Fig. 9). It represents the flooding of the lowest peat bed found in the Mad River slough (Fig. 5) and is about 300 cm below the modern surface. While no stumps are present, tree roots are found on this buried bed in the Mad River slough. In southern Humboldt Bay, ambiguous foraminiferal assemblages indicate both a good RSL rise (Ia–II; 25–50 cm) and a minor RSL fall (Ib–Ia; −25–0 cm). In the Eel River delta, foraminiferal assemblages across the bed 3 contact (250 cm) indicate an RSL rise (Ia–III; > 75 cm).

Magnitude of Submergence Event E5(?). The stratigraphy of the Mad River slough and one of the locations in southern Humboldt Bay contains evidence for submergence event E5(?); see Table 5 and Figure 9. However, the evidence for coseismic subsidence is not unequivocal (Table 5). The Little Salmon fault ruptured within this range (> 1520–1820 cal B.P.; < 1820–2114 cal B.P.; Carver and McCalpin, 1996), which could be assigned to this submergence event, E5(?), or to submergence event E6. Submerged roots in the Mad River slough indicate that the buried peat bed was above higher high water prior to submergence into the intertidal zone. While this does not require coseismic subsidence, the submergence of woodlands into the intertidal zone supports an earthquake cause. Some evidence has been found for earthquakes in other locations during this time period (e.g., Darienzo and Peterson, 1990; Nelson *et al.*, 2008; Goldfinger *et al.*, 2012), but considering its proximity in time with submergence event E6, this evidence cannot be unequivocally tied to submergence event E5(?). However, Darienzo and Peterson (1990) did find evidence for two closely spaced earthquakes during this time period. The ambiguous elevation changes observed could be explained by a local earthquake (M_w 6.5–7.2), only causing minor submergence in southern Humboldt Bay and greater submergence in the Mad River slough. Our preferred interpretation is that rupture of the Little Salmon fault or a coincidental local RSL change caused submergence event E5(?).

Submergence Event E6 (1750–1900 cal B.P.; Regional).

Evidence for Submergence Event E6. Submergence event E6 is the oldest submergence event for which there is enough preserved stratigraphy and other information to evaluate its potential sources (Table 6 and Fig. 9). Submergence event E6 is older than the lowest documented stratigraphy in the Mad River slough. There are buried beds within this age range at Eureka, southern Humboldt Bay, and Eel River. The RSL data from southern Humboldt Bay shows good evidence of a buildup of the surface (from zone III to I) but only a minor RSL rise (I–II; 0–50 cm) at the contact. The Eel River delta foraminiferal stratigraphy shows good evidence of an RSL rise (I–III; > 50 cm).

Magnitude of Submergence Event E6. Although evidence for this submergence event is only found in the Eel River delta and southern Humboldt Bay (Table 6 and Fig. 9), a regional earthquake ($M_w \sim 8.2$) is proposed based on the magnitude of environmental changes observed in the Eel River delta. The absence of submergence event E6 in the Mad River slough record is due to the relatively short length of its record, which does not extend back to this time period. Submergence event E6 potentially represents an entire CSZ rupture. The Little Salmon fault ruptured within this range (> 1520–1820 cal B.P.; < 1820–2114 cal B.P.), but our preferred interpretation is that the rupture of this fault caused submergence event E5(?). Earthquake proxies with similar ages are found in the offshore turbidite record (Goldfinger *et al.*, 2012) and estuaries all along the Pacific Northwest coast including Coos Bay (Nelson *et al.*, 1996), Bradley Lake (Kelsey *et al.*, 2005), and Coquille River (Witter *et al.*, 2003) in Oregon, and Grays Harbor, Copalis River, and Willipa Bay in Washington (Atwater, 1987; Shennan *et al.*, 1996; Atwater *et al.*, 2004; Table 6).

Conclusions

The Quaternary stratigraphy of Humboldt Bay and the Eel River delta contains evidence for between four and six earthquakes. The submergence events and timing of other paleoseismic records support the hypothesis that two or three of the six submergence events were caused by local earthquakes and that three or four of the six submergence events were either regional or entire subduction zone earthquakes. This is important because it suggests that not all coseismic submergence events are associated with the rupture of the subduction zone megathrust and that faults in the upper plate, like the Little Salmon fault, may rupture coseismically with large earthquakes on the subduction zone megathrust. Individual faults of the upper plate can rupture and therefore cause major earthquakes, independent of the underlying subduction zone megathrust.

Establishing the fact that the rupture occurred along the entire subduction zone at the exact same time is problematic. However, using multiple ^{14}C ages, dendrochronology, and a tsunami report in Japan, other researchers have built a strong case that the most recent earthquake ruptured the entire length of the subduction zone about 300 years ago. The correlation between sites along the entire subduction zone for older earthquakes is more problematic. The uncertainties in the age correlation do not rule out the possibility that the timing of some coseismic submergence events may correlate with earthquakes along the CSZ in Oregon and Washington.

Data and Resources

The data used in this report came from Ⓔ sedimentological descriptions of outcrops and cores, which are available as an electronic supplement to this paper. A copy of Ⓔ all ^{14}C ages are available in the electronic supplement to this paper. The original descriptions used in this paper can be obtained by contacting David Valentine.

Acknowledgments

The authors would like to thank Brian Atwater and Art Sylvester for reviewing earlier versions of this manuscript. Alan Nelson, an anonymous reviewer, and Associate Editor Brian Sherrod provided excellent comments during the formal review. We would also like to acknowledge the U.S. Geological Survey (USGS) for financial support of this work.

References

Abramson, H. (1998). Evidence for tsunamis and earthquakes during the last 3500 years from Lagoon Creek, a coastal freshwater marsh, northern California, *Master's Thesis*, Humboldt State University, Arcata, California, 76 pp.

Adams, J. (1990). Paleoseismicity of the Cascadia subduction zone: Evidence from turbidites off the Oregon-Washington margin, *Tectonics* **9,** 569–583.

Ammon, C. J., C. Ji, H.-K. Thio, D. Robinson, S. Ni, V. Hjorleifsdottir, H. Kanamori, T. Lay, S. Das, D. Helmberger, G. Ichinose, J. Polet, and D. Wald (2005). Rupture process of the 2004 Sumatra-Andaman earthquake, *Science* **308,** 1133–1139.

Atwater, B. F. (1987). Evidence for great Holocene earthquakes along the outer coast of Washington state, *Science* **236,** no. 4804, 942–944.

Atwater, B. F. (1992). Geologic evidence for earthquakes during the past 2000 yr along the Copalis River, south coastal Washington, *J. Geophys. Res.* **97,** 1901–1919.

Atwater, B. F., and E. Hemphill-Haley (1997). Recurrence intervals for great earthquakes of the past 3500 years at northeastern Willapa Bay, Washington, *U.S. Geol. Surv. Profess. Pap.*, 108 pp.

Atwater, B., M. Stuiver, and D. Yamaguchi (1991). Radiocarbon test of earthquake magnitude at the Cascadia subduction zone, *Nature* **353,** no. 6340, 156–158.

Atwater, B. F., M. P. Tuttle, E. S. Schweig, C. M. Rubin, D. K. Yamaguchi, and E. Hemphill-Haley (2004). Earthquake reoccurrence inferred from paleosiesmology, in *The Quaternary Period in the United States: Developments in Quaternary Science*, A. R. Gillespie, S. C. Porter, and B. F. Atwater (Editors), Elsevier, New York, 331–350.

Burger, R. L., C. S. Fulthorpe, J. A. Austin Jr., and S. P. S. Gulick (2002). Lower Pleistocene to present structural deformation and sequence stratigraphy of the continental shelf, offshore Eel River Basin, northern California, *Mar. Geol.* **185,** 249–281.

Carver, G. A. (1992). Late Cenozoic tectonics of coastal northern California, in *Field Guide to the Late Cenozoic Subduction Tectonics and Sedimentation of Northern California*, GB-71, Pacific Section, G. A. Carver and K. R. Alto (Editors), American Association of Petroleum Geologists, Bakersfield, California, pp. 1–11.

Carver, G. A., and J. McCalpin (1996). Paleoseismology in compressional tectonic environments, in *Paleoseismology: International Geophysics Series*, J. McCalpin (Editor), Academic Press, San Diego, California, 183–270.

Carver, G. A., H. A. Abramson, C. E. Garrison-Laney, and T. Leroy (1999). Paleotsunami evidence from northern California for repeated long rupture (M 9) of the Cascadia subduction zone, *Sesimol. Res. Lett.* **20,** no. 2, p. 232.

Cifuentes, I. L. (1989). The 1960 Chilean earthquake, *J. Geophys. Res.* **94,** 665–680.

Clague, J. J., B. F. Atwater, K. Wang, Y. Wang, and I. Wong (2000). *Program Summary and Abstracts of the Geological Society of America Penrose Conference 2000, Great Cascadia Earthquake Tricentennial*, Seaside, Oregon, 2–8 June 2000, Oregon Department of Geology and Mineral Industries, 1–156.

Clague, J. J., T. Bobrowsky, and I. Hutchison (2000). A review of geological records of large tsunamis at Vancouver Island, British Columbia, and implications for hazard, *Quat. Sci. Rev.* **19,** 849–863.

Clarke, S. H., Jr. (1992). Geology of the Eel River Basin and adjacent region: Implications for Late Cenozoic tectonics of the southern Cascadia subduction zone and Mendocino triple junction, *Am. Assoc. Petrol. Geol. Bull.* **76,** 199–224.

Clarke, S. H., and G. A. Carver (1992). Late Holocene tectonics and paleoseismicity, southern Cascadia subduction zone, *Science* **255,** 188–192.

Cronin, T. M., P. R. Vogt, D. A. Willard, R. Thunell, J. Halka, M. Berke, and J. Pohlman (2007). Rapid sea level rise and ice sheet response to 8,200-year climate event, *Geophys. Res. Lett.* **34,** doi 10.1029/2007GL031318.

Darienzo, M. E., and C. D. Peterson (1990). Episodic tectonic subsidence of late Holocene salt marshes, northern Oregon central Cascadia margin, *Tectonics* **9,** no. 1, 1–22.

Darienzo, M. E., C. D. Peterson, and C. Clough (1994). Stratigraphic evidence for great subduction-zone earthquakes at four estuaries in northern Oregon, U.S.A., *J. Coast. Res.* **10,** no. 4, 850–876.

Dengler, L. A., G. A. Carver, and B. C. McPherson (1991). Potential sources of large earthquakes in north coastal California, in *Proc. of the AGU 1991 Fall Meeting*, Eos Trans. AGU, San Francisco, California, 9–13 December 1991, p. 315.

Eicher, A. L. (1987). Salt marsh vascular plant distribution in relation to tidal elevation, Humboldt Bay, California, *Master's Thesis*, Humboldt State University, Arcata, California, 78 pp.

Goldfinger, C., C. H. Nelson, J. E. Johnson, and The Shipboard Scientific Party (2003). Holocene earthquake records from the Cascadia subduction zone and northern San Andreas fault based on precise dating of offshore turbidites, *Annu. Rev. Earth Planet. Sci.* **31,** 555–571.

Goldfinger, C., C. H. Nelson, A. E. Morey, J. E. Johnson, J. Patton, E. Karabanov, J. Gutiérrez-Pastor, A. T. Eriksson, E. Gràcia, G. Dunhill, R. J. Enkin, A. Dallimore, and T. Vallier (2012). Turbidite event history—Methods and implications for Holocene paleoseismicity of the Cascadia subduction zone, *U.S. Geol. Surv. Profess. Pap. 1661-F*, 170 pp., available at http://pubs.usgs.gov/pp/pp1661f/.

Hawkes, A. D., B. P. Horton, A. R. Nelson, and D. F. Hill (2010). The application of intertidal foraminifera to reconstruct coastal subsidence during the giant Cascadia earthquake of AD 1700 in Oregon, USA, *Quat. Int.* **221,** 116–140.

Hawkes, A.D., B. P. Horton, A. R. Nelson, C. H. Vane, and Y. Sawai (2011). Coastal subsidence in Oregon, USA, during the giant Cascadia earthquake of AD 1700, *Quat. Sci. Rev.* **30,** 364–376.

Heaton, T. H., and H. Kanamori (1984). Seismic potential associated with subduction in the northwestern United States, *Bull. Seismol. Soc. Am.* **74,** 933–941.

Jacoby, G. C., C. Carver, and W. Wagner (1995). Trees and herbs killed by an earthquake 300 yrs ago at Humboldt Bay, California, *Geology* **29,** 77–80.

Jennings, A. E., and A. R. Nelson (1992). Foraminiferal assemblage zones in Oregon tidal marshes; relation to marsh floral zones and sea level, *J. Foraminiferal Res.* **22,** no. 1, 13–29.

Kelsey, H. M., A. R. Nelson, E. Hemphill-Haley, and R. C. Witter (2005). Tsunami history of an Oregon coastal lake reveals a 4600 yr record of great earthquakes on the Cascadia subduction zone, *Geol. Soc. Am. Bull.* **117,** 1009–1032.

Kelsey, H. M., R. C. Witter, and E. Hemphill-Haley (1998). Response of a small Oregon estuary to coseismic subsidence and postseismic uplift in the past 300 years, *Geology* **26,** 231–234.

Kelsey, H. M., R. C. Witter, and E. Hemphill-Haley (2002). Plate-boundary earthquakes and tsunamis of the past 5500 yr, Sizes River estuary, southern Oregon, *Geol. Soc. Am. Bull.* **114,** 298–314.

Kittelson, P. M., and M. J. Boyd (1997). Mechanisms of expansion for an introduced species of cordgrass, Spartina densiflora, in Humboldt Bay, California, *Estuaries* **20,** 770–778.

Leonard, L. J., C. A. Currie, S. Mazzotti, and R. D. Hyndman (2010). Rupture area and displacement of past Cascadia great earthquakes from coastal coseismic subsidence, *Geol. Soc. Am. Bull.* **122,** 2079–2096.

Li, W. H. (1992). Evidence for the late Holocene coseismic subsidence in the Lower Eel River valley, Humboldt county, Northern California: An application of foraminiferal zonation to indicate tectonic submergence, *Master's thesis*, Humboldt State University.

Manhart, C. S. (1992). High resolution Foraminiferid stratigraphy as evidence for rapid, coseismic subsidence: Preliminary results, in *Field Guide to the Late Cenozoic Subduction Tectonics and Sedimentation of Northern Coastal California*, Pacific Section, American Association of Petroleum Geologists, Bakersfield, California, 39–44.

McCalpin, J. P., and A. R. Nelson (1996). Introduction to paleoseismology, in *Paleoseismology: International Geophysics Series*, J. McCalpin (Editor), Academic Press, San Diego, California, 1–32.

McCory, P. A. (1996). Evaluation of fault hazards, northern coastal California, *U.S. Geol. Surv. Open File Rept. 96–656*, 87 pp.

Merritts, D., and W. B. Bull (1989). Interpreting quaternary uplift rates at the Mendocino Triple Junction, northern California, *Geology* **17,** 1020–1024.

Muir-Wood, R. (1989). The November 7th 1837 earthquake in southern Chile, *Seismol. Res. Lett.* **60,** no. 1, p. 8.

Nelson, A. R. (1992). Holocene tidal-marsh stratigraphy in south central Oregon—evidence of localized subsidence in the Cascadia subduction zone, in *Quaternary Coast of the United States: Marine and Lacustrine systems*, Society for Sedimentary Research (SEPM) Special Publication 48, C. Fletcher and J. F. Wehmiler (Editors), Society for Sedimentary Research, Tulsa, Oklahoma, 287–302.

Nelson, A. R., B. F. Atwater, P. T. Bobrowsky, L.-A. Bradley, J. J. Clague, G. A. Carver, M. E. Darienzo, W. C. Grant, H. W. Krueger, R. Sparks, T.W. Stafford Jr., and M. Stuiver (1995). Radiocarbon evidence for extensive plate-boundary rupture about 300 years ago at the Cascadia subduction zone, *Nature* **378,** 371–374.

Nelson, A. R., H. M. Kelsey, and R. C. Witter (2006). Great earthquakes of variable magnitude at the Cascadia subduction zone, *Quat. Res.* **65,** 354–365.

Nelson, A. R., Y. Ota, M. Umitsu, K. Kashima, and Y. Matsushima (1998). Seismic or hydrodynamic control of rapid late-Holocene sea-level rises in southern coastal Oregon, USA?, *The Holocene* **8,** 287–299.

Nelson, A. R., Y. Sawaki, A. E. Jennings, L.-A. Bradley, L. Gerson, B. L. Sherrod, J. Sabean, and B. P. Horton (2008). Great-earthquake paleogeodesy and tsunamis of the past 2000 years at Alsea Bay, central Oregon coast, USA, *Quat. Sci. Rev.* **27,** 747–768.

Nelson, A. R., I. Shennan, and A. J. Long (1996). Identifying coseismic subsidence in tidal-wetland stratigraphic sequences at the Cascadia subduction zone of western North America, *J. Geophys. Res.* **101,** 6115–6135.

Oppenheimer, D., G. Beroza, G. Carver, L. Dengler, J. Eaton, L. Gee, F. Gonzalez, A. Jayko, W. H. Li, M. Lisowski, M. Magee, G. Marshall, M. R. Murray, B. McPherson, B. Romanowicz, K. Satake, R. Simpson, P. Somerville, R. Stein, and D. Valentine (1993). The Cape Mendocino, California, earthquakes of April 1992: Subduction at the triple junction, *Science* **261,** 433–438.

Reimer, P. J., M. G. L. Baillie, E. Bard, A. Bayliss, J. W. Beck, P. G. Blackwell, C. Bronk Ramsey, C. E. Buck, G. S. Burr, R. L. Edwards, M. Friedrich, P. M. Grootes, T. P. Guilderson, I. Hajdas, T. J. Heaton, A. G. Hogg, K. A. Hughen, K. F. Kaiser, B. Kromer, F. G. McCormac, S. W. Manning, R. W. Reimer, D. A. Richards, J. R. Southon, S. Talamo, C. S. M. Turney, J. van der Plicht, and C. E. Weyhenmeyer (2009). IntCal09 and Marine09 radiocarbon age calibration curves, 0–50,000 years cal BP, *Radiocarbon* **51,** no. 4, 1111–1150.

Satake, K., K. Shimazaki, Y. Tsuji, and K. Udeda (1996). Time and size of a giant earthquake in the Cascadia inferred from Japanese tsunami records of January 1700, *Nature* **379,** 246–249.

Schlichting, R. B., and C. D. Peterson (2006). Mapped overland distance of paleotsunami high-velocity inundation in back-barrier wetlands of the central Cascadia margin, USA, *J. Geology* **114,** 577–592.

Scott, D. B., and F. S. Medioli (1986). Foraminifera as sea-level indicators, in *Sea-Level Research: A Manual for the Collection and Evaluation of Data*, GeoBooks, Norwich, Great Britain, 435–455.

Scott, D., E. Collins, J. Duggan, A. Asioli, T. Saito, and S. Hasewaga (1996). Pacific Rim marsh foraminiferal distributions: Implications for sea-level studies, *J. Coast. Res.* **12,** no. 4, 850–861.

Shennan, I., A. J. Long, M. M. Rutherford, F. M. Green, J. B. Innes, J. M. Lloyd, U. Zong, and K. J. Walker (1996). Tidal marsh stratigraphy, sea-level change and large earthquakes, I: A5000 year record in Washington, U.S.A., *Quat. Sci. Rev.* **15,** 1023–1059.

Shennan, I., A. J. Long, M. M. Rutherford, J. B. Innes, F. M. Green, and K. J. Walker (1998). Tidal marsh stratigraphy, sea-level change and large earthquakes, II: Submergence events during the alst 3500 years at Netarts Bay, Oregon, USA, *Quat. Sci. Rev.* **17,** 365–393.

Shivelle, C. D., G. A. Carver, and D. W. Valentine (1991). Foraminiferid stratigraphy as evidence for great earthquakes on the Cascadia subduction zone in Northern California, in *Geological Society of America Abstracts with Programs*, Vol. **23**, Geological Society of America, Boulder, Colorado, p. 97.

Toppozada, T., G. Borchardt, W. Haydon, M. Petersen, R. Olson, H. Lagorio, and T. Anvik (1995). *Planning Scenario in Humboldt and Del Norte Counties, California for a Great Earthquake on the Cascadia Subduction Zone*, Special Publication, California Division of Mines and Geology, Sacramento, California, 151 pp.

Valentine, D. W. (1992). Late Holocene stratigraphy and paleoseismicity, Humboldt Bay, California, *Master's Thesis* Humboldt State University, 82 pp.

Verdonk, D. (1995). Three-dimensional model of vertical deformation at the southern Cascadia subduction zone, western United States, *Geology* **23,** no. 3, 261–264.

Vick, G. (1988). Late Holocene paleoseismicity and relative vertical crustal movements, Mad River slough, Humboldt Bay, California, *Master's Thesis*, Humboldt State University, 88 pp.

Vigny, C., A. Socquet, S. Peyrat, J. C. Ruegg, M. Metois, R. Madariaga, S. Morvan, M. Lancieri, R. Lacassin, J. Campos, D. Carrizo, M. Bejar-Pizarro, S. Barrientos, R. Armijo, C. Aranda, M.-C. Valderas-Bermego, I. Ortega, F. Bondoux, S. Baize, H. Lyon-Caen, A. Pavez, J. P. Vilotte, M. Bevis, B. Brooks, R. Smalley, H. Parra, J.-C. Baez, M. Blanco, S. Cimbaro, and E. Kendrick (2011). The 2010 M_w 8.8 Maule megathrust earthquake of central Chile, monitored by GPS, *Science* **332,** 1417–1421.

Wells, D. L., and J. K. Coppersmith (1994). New empirical relationships among magnitude, rupture length, rupture width, rupture area, and surface displacement, *Bull. Seismol. Soc. Am.* **84,** no. 4, 974–1002.

Witter, R. C., H. M. Kelsey, and E. Hemphill-Haley (2003). Great Cascadia earthquakes and tsunamis of the past 6700 years, Coquille River estuary, southern coastal Oregon, *Geol. Soc. Am. Bull.* **115,** 1289–1306.

University of California, San Diego
San Diego Supercomputer Center, MC 0505
9500 Gilman Drive
La Jolla, California 92093-0505
david.valentine@gmail.com
(D.W.V.)

Department of Earth Science
University of California, Santa Barbara
1006 Webb Hall
Santa Barbara, California 93106
ed.keller@geol.ucsb.edu
asimms@geol.ucsb.edu
(E.A.K., A.R.S.)

Department of Geology
Humboldt State University
1 Harpst St.
Arcata, California 95521
cgeol@acsalaska.net
(G.C.)

Northrop Grumman Co.
3643 Doolittle Dr.
Redondo Beach, California 90278
whl222@msn.com
(W.-H.L.)

Environmental Services and Consulting
P.O. Box 11437
Blacksburg, Virginia 24062
Christine.manhart@gmail.com
(C.M.)

Manuscript received 7 April 2011